DOSE VALIDATION OF ACCELERATED PARTIAL BREAST IRRADIATION TREATED WITH THE SAVI APPLICATOR

by

Janeil K. Pinder

A Thesis Submitted to the Faculty of

The Charles E. Schmidt College of Science

In Partial Fulfillment of the Requirements for the Degree of

Professional Science Master

Florida Atlantic University

Boca Raton, FL

December 2017

DOSE VALIDATION OF ACCELERATED PARTIAL BREAST IRRADIATION

TREATED WITH THE SAVI APPLICATOR

by

Janeil K. Pinder

This thesis was prepared under the direction of the candidate's thesis co-advisors, Dr. Silvia Pella, and Dr. Theodora Leventouri, Department of Physics, and has been approved by the members of her supervisory committee. It was submitted to the faculty of the Charles E. Schmidt College of Science and was accepted in partial fulfillment of the requirements for the degree of Professional Science Master.

SUPERVISORY COMMITTEE:

Silvia Pella, Ph.D., DABR
Thesis Co-Advisor

Theodora Leventouri, Ph.D.
Thesis Co-Advisor

Zoubir Ouhib, MS, DABR, FACR

Georgios Kalantzis, Ph.D.

Luc T. Wille, Ph.D.
Chair, Department of Physics

Ata Sarajedini, Ph.D.
Dean, Charles E. Schmidt College of Science

Deborah L. Floyd, Ed.D.
Dean, Graduate College

December 5, 2017
Date

ACKNOWLEDGEMENTS

First and foremost, I would like to give recognition to God, for His grace and mercy. I would not have made it this far without His favor over my life.

I would like to express my gratitude to Dr. Silvia Pella, my thesis advisor, for her clinical guidance, patience, and support. Thank you for committing to my success, sticking with me, and never giving up on me.

A heart felt thank you to Dr. Theodora Leventouri, the program director, whom has been an inspiration to me. Thank you for the continuous encouragement and support during my years of study.

Also, I would like to acknowledge the faculty and staff of Florida Atlantic University, as well as my fellow classmates who contributed to this research and data collection.

Special thanks to the staff of South Florida Radiation Oncology/21st Century Oncology for providing me access to their facilities, equipment and software. As well as 21st Century Oncology TLD Lab, for providing, calibrating and reading the TLD chips, and .decimal, Inc. (dot decimal) for providing the 3D phantom.

Finally, thank you to my family, friends, the Cathedral of Praise Church of God community, and the Bahamian community for their moral and financial support that helped me throughout my pursuit of a higher education. It has not gone unnoticed.

ABSTRACT

Author: Janeil K. Pinder

Title: Dose Validation for Partial Accelerated Breast Irradiation treated with the SAVI Applicator

Institution: Florida Atlantic University

Thesis Advisors: Silvia Pella, Ph.D., DABR and Theodora Leventouri, Ph.D.

Degree: Professional Science Master

Year: 2017

The purpose of this study is to verify and validate the dose at various points of interest in accelerated partial breast irradiation (APBI) treated with the Strut Adjusted Volume Implant (SAVI) applicator using Thermoluminescent Dosimeters (TLDs). A set of CT images were selected from a patient's data who had received APBI using the SAVI applicator. The images were used to make 3D models. TLDs were calibrated for Brachytherapy. Various points of interest were marked out and slots were carved in the 3D models to fit the TLDs. CT scans were taken of the 3D models with expanded SAVI applicator inserted. A plan was made following B-39 protocol. The TLDs were read and the absorbed doses were calculated and compared to the delivered doses. The results of this study show that the overall average reading of the TLDs is within expected value. The TPS shows overestimated dose calculations for brachytherapy.

In Loving Memory of Sis. Keturah Wright and Sis. Colette Newry-Machaliwa

DOSE VALIDATION OF ACCELERATED PARTIAL BREAST IRRADIATION TREATED WITH THE SAVI APPLICATOR

LIST OF TABLES

LIST OF FIGRES

1. INTRODUCTION

1.1 Purpose

The purpose of this study is to verify and validate the calculated dose at various points in a brachytherapy planning using high dose rate (HDR) irradiation for an accelerated partial breast irradiation (APBI) treated with the Strut Adjusted Volume Implant (SAVI) applicator. The dosimetric verification will be made with Thermoluminescent Dosimeters (TLDs). The TLDs should be calibrated and corrected specifically for the isotope used in the brachytherapy treatment; in this study Ir-192 was used. The TLDs will be use as reference dose readings. The readings will be made at preset points where the dose was calculated by Oncentra treatment planning system (TPS). Oncentra's dose calculations follows American Association of Physicists in Medicine (AAPM) Task Group 43 (TG-43) recommended dose calculations which does not correct for any inhomogeneity. The acceptable tolerance for in-vivo dosimetry in HDR brachytherapy treatment is ±10%.

1.2 The Anatomy of the Female Breast

The breast is the tissue overlying the chest muscles. Women's breasts are made of specialized tissue that produces milk (glandular tissue) as well as fatty tissue. The amount of fat determines the size of the breast. The milk-producing part of the breast is organized into 15 to 20 sections, called lobes. Within each lobe are smaller structures, called lobules, where milk is produced. The milk travels through a network of tiny tubes called ducts. The

ducts connect and come together into larger ducts, which eventually exit the skin in the nipple. The dark area of skin surrounding the nipple is called the areola.

Connective tissue and ligaments provide support to the breast and give it its shape. Nerves provide sensation to the breast. There are blood vessels and lymphatics in the breast. The lymphatics are thin channels similar to blood vessels; they do not carry blood but collect and carry tissue fluid which ultimately reenters the blood stream. Breast tissue fluid drains through the lymphatics into the lymph nodes located in the underarm (axilla) and behind the breast bone (sternum) [1] [2].

(Source: The National Cancer Institute)

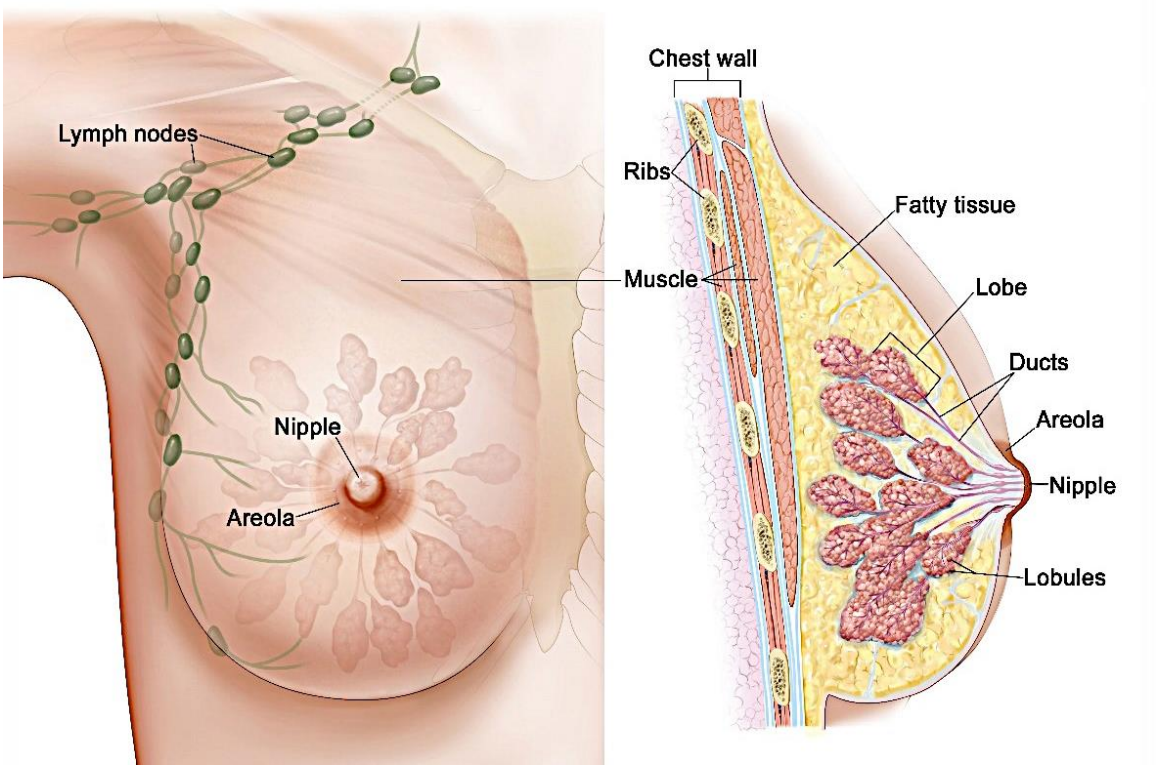

Figure 1: Anatomy of the female breast.

Left) The nipple and areola are shown on the outside of the breast.

Right) The lymph nodes, lobes, lobules, ducts, and other parts of the inside of the breast [3].

1.3 Breast Cancer

Breast cancer occurs when cells in the breast grow out of control and form a growth or tumor. The tumor may be malignant (cancerous) or benign (non-cancerous). There are two forms of malignant breast cancer:

- Invasive breast cancer is when cancerous cells spread to other parts of the body through the bloodstream and lymph nodes.
- Noninvasive breast cancer is when cancerous cells remain in the breast, and do not spread to surrounding tissue, lobules or ducts [4].

In the U.S., breast cancer is the second most common cancer in women after skin cancer. It can occur in both men and women, but it is rare in men. Each year there are about 100 times more new cases of breast cancer in women than in men [3].

1.3.1 Staging of Breast Cancer

Breast cancer is staged using specific criteria known as the Tumor, Node, and Metastases (TNM) staging system. This system is determined by The American Joint Committee on Cancer (AJCC). The T category describes the size of the tumor. The N category describes if there are lymph nodes involved. The M category tells if there were any distant metastases (spread).

Once the T, N, and M are determined, they are combined, and an overall stage of Stage 0, I, IIA, IIB, IIIA, IIIB, IIIC, or IV can be diagnosed, as shown in Table 1.

Table 1: Stages of Breast Cancer [5] [6].

Stage	T N M			Definition
0	T_{is}	N_0	M_0	Cancer cells remain inside the breast duct, without spreading.
IA	T_1	N_0	M_0	Tumor (in the breast) ≤ 2 cm And Cancer cells have not spread outside the breast (no lymph nodes are involved).
IB	T_{0-1}	N_{1mi}	M_0	No tumor in the breast **OR** Tumor (in the breast) ≤ 2 cm And 0.2mm ≤ Cancer cells (in the lymph nodes) ≤ 2 mm.
IIA	T_{0-1} T_2	N_1 N_0	M_0 M_0	No tumor in the breast **OR** Tumor (in the breast) ≤ 2 cm And Cancer cells are found in the axillary lymph nodes **OR** 2 cm ≤ Tumor (in the breast) ≤ 5 cm And Cancer cells have not spread to the axillary lymph nodes.
IIB	T_2 T_3	N_1 N_0	M_0 M_0	2 cm ≤ Tumor (in the breast) ≤ 5 cm And Cancer cells have spread to the axillary lymph nodes **OR** Tumor (in the beast) ≥ 5 cm But Cancer cells have not spread to the axillary lymph nodes.
IIIA	T_{0-2} T_3	N_2 N_{1-2}	M_0 M_0	No tumor in the breast **OR** Tumor (in the breast) is any size And Cancer cells have spread to the axillary lymph nodes, which are sticking together or to other structures, or cancer may be found in lymph nodes near the breastbone.
IIIB	T_4	N_{0-2}	M_0	Tumor (in the breast) is any size And Cancer cells have spread to the chest wall and/or skin of the breast and may have spread to axillary lymph nodes that are clumped together or sticking to other structures or cancer may have spread to lymph nodes near the breastbone.
IIIC	T_{Any}	N_3	M_0	No tumor in the breast **OR** Tumor (in the breast) is any size. And Cancer cells may have spread to the chest wall and/or the skin of the breast, lymph nodes either above or below the collarbone, or to axillary lymph nodes or lymph nodes near the breastbone.
IV	T_{Any}	N_{Any}	M_1	Cancer cells have spread or metastasized.

1.3.2 Naming of Breast Cancer

Breast cancer is named base on its origin, and its spread. Breast cancer can begin in different areas of the breast such as in ducts, lobules, or the tissue in between. If it originates in the cells that lines the organ or tissue, it is considered *carcinoma*. If it originates in the cells that make glands, it is considered *adenocarcinoma*. If it originates in the cells of the muscle, fat or connective tissue, it is considered *sarcoma*. If the cancer has spread to surrounding areas, it is considered *invasive or infiltrating*. If it has not spread, it is considered *in situ*.

Breast cancer can also be considered *recurrent*. This means the cancer has return, after the detection period, in the same or opposite breast, or chest wall.

Table 2: Common Types of Breast Cancer [6] [7].

Types	Definition
Ductal Carcinoma in Situ (DCIS)	Cancer that starts inside the milk ducts and has not spread beyond the milk duct.
Invasive/Infiltrating Ductal Carcinoma (IDC)	Cancer that has broken through the wall of the milk duct and begun to invade the tissues of the breast.
Tubular Carcinoma of the Breast (IDC Subtype)	The tumor is usually small (≤1 cm) and is made up of tube-shaped structures called "tubules."
Medullary Carcinoma of the Breast (IDC Type)	The tumor is a soft, fleshy mass that resembles a part of the brain called the medulla.
Mucinous/Colloid Carcinoma of the Breast (IDC Type)	The tumor is made up of abnormal cells that “float” in pools of mucin.
Papillary Carcinoma of the Breast (IDC Type)	The tumor usually has a well-defined border and is made up of small, finger-like projections.
Invasive/Infiltrating Lobular Carcinoma (ILC)	Cancer that has broken through the wall of the lobule and begun to invade the tissues of the breast.
Lobular Carcinoma in Situ (LCIS)	An area of abnormal cell growth that increases a person’s risk of developing invasive breast cancer later in life.

1.4 Treatment of Breast Cancer

When treating breast cancer, the oncologist will determine the type of treatment based on the type breast cancer, the stage, the size of the tumor and the hormone sensitivity of the cells. Most women will have their tumor surgically removed along with either chemotherapy, hormone therapy, biological therapy, radiation therapy or a combination of therapies.

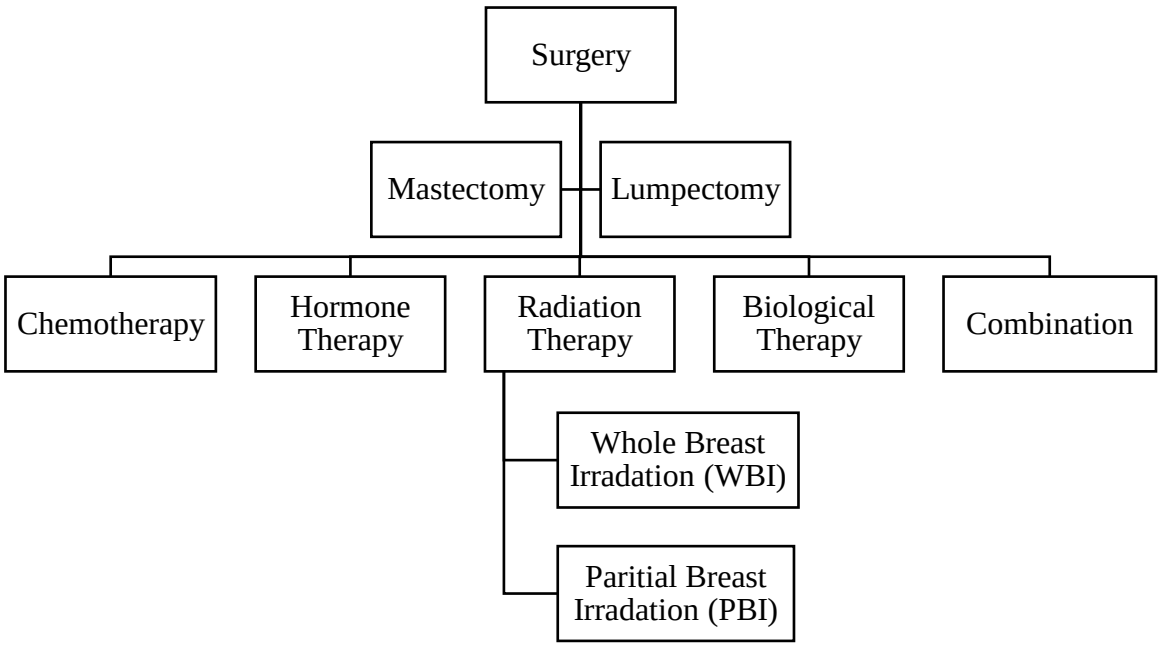

Figure 2: Schematic representation of breast cancer treatment options.

1.4.1 Surgery

Traditional Mastectomy

A mastectomy consists of the surgical removal of the entire breast, along with the muscles of the chest wall, and the axillary lymph nodes. Prior to the 1970s, the treatment of breast cancer was dominated by radical mastectomy or modified radical mastectomy of the affected breast. This was advocated as the most appropriate local therapy for women with early-stage breast cancers [8].

Breast Conservation Surgery

The goal of Breast Conservation Therapy (BCT) is to preserve, as much as possible, healthy breast tissues. To accomplish this, women now have the option to receive Breast conserving surgery (BCS). This is also referred to as lumpectomy, quadrantectomy, partial mastectomy, or segmental mastectomy. BCS is followed by whole breast irradiation (WBI) or partial breast irradiation (PBI).

Studies have found equivalent survival and local control rates among women treated with BCT compared to those treated with mastectomy. As well as, equivalent results with women treated with PBI as women treated with WBI, even though WBI is consider the standard care for women with stage 0, I and II breast cancer [8] [9] [10].

1.4.2 Radiation Therapy

Radiation therapy is a cancer treatment that uses ionizing radiation to kill cancer cells or keep them from growing. This is done by impairing the DNA of the cancer cells and their ability to regenerate. The damage to the DNA can be caused by direct or indirect ionizing radiation. Direct ionizing radiation uses charged particles to break chemical bonds and indirect ionizing radiation uses photons interactions to create oxygen free-radical. Because radiation therapy can damage both cancer cells and normal cell, the goal of radiation therapy is to deliver the maximum of radiation needed to kill the cancer, while sparing normal tissue [11]. Radiation therapy can be delivered in three forms:

- *Externally* which uses a machine outside the body to send high energy radiation towards the cancer, it is the most used type of radiation therapy and is also referred to as External Beam Radiation Therapy.

- *Internally* which uses a radioactive substance sealed in needles, seeds, wires, or catheters that are placed directly into or near the cancer. This form of radiation therapy is most commonly referred to as Brachytherapy.
- *Systemic* which administers radioactive materials orally or through a vein. The material travels throughout the body and gives off radiation after it attaches to the cancer cells. The radiation becomes weaker and eventually passes through the body.

External Beam Radiation Therapy

External beam radiation therapy (EBRT) is a treatment which utilizes Linear Accelerator (Linac) to target tumors anywhere in the body, whiles sparing normal tissue. The Linac generates the beam by using a waveguide to accelerate radiation particles guided by magnetic fields. When the particles hit a tungsten target at the end of the waveguide, a beam is created. These particles can be made of either electrons, photons or protons. The beam is then shaped with blocks or collimators to outline the treatment area.

Brachytherapy

The term "brachy" is Greek for short distance. Brachytherapy is a treatment which utilizes radioactive material that is implanted in the tumor (interstitial) or within a very close range (intracavitary) of the tumor. It is the first and most conformal radiation therapy.

Some examples of the radioactive materials used are Cesium-131, Cesium-137, Cobalt-60, Iridium-192, Iodine-125, Palladium-103, Ruthenim-106, or Radium-226. These materials can be delivered through two methods: Hot loading or Afterloading. Hot loading is when the applicator contains the radioactive material at the time of implant and afterloading is delivering the radioactive material after the applicator is implanted.

During delivery, the implants can be within the patient temporary, ranging from a few minutes to days, or permanently. The dose rate can range from Low-dose Rate (LDR, ≤ 2 Gy/hr), Medium-dose Rate (MDR, 2 Gy/hr - 12 Gy/hr), High-dose Rate (HDR, 12 Gy/hr ≤), or Pulsed-Dose Rate (PDR).

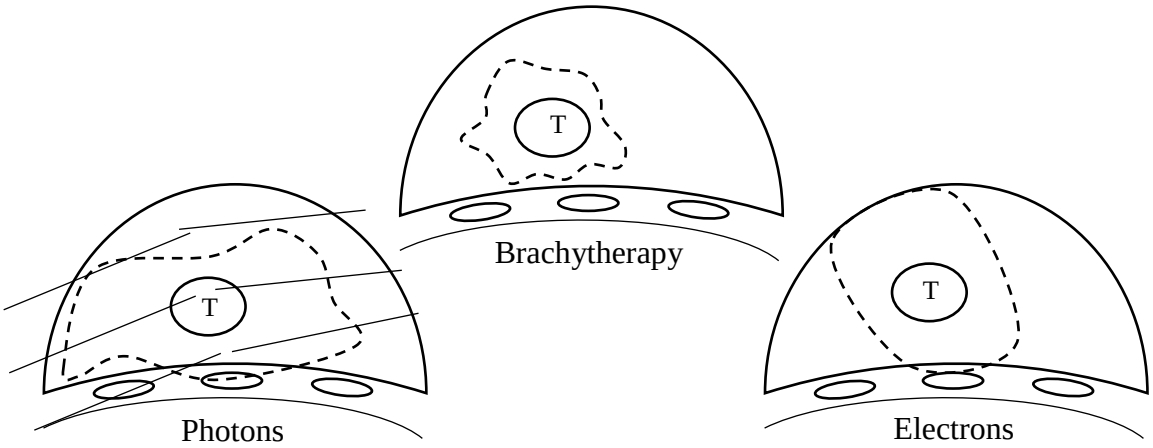

Figure 3: Conformal dose coverage comparison of the breast with 3 different modes of delivering dose. A) Photons, B) Brachytherapy, C) Electrons.

1.5 Accelerated Partial Breast Irradiation

Accelerated partial breast irradiation (APBI) is a curative approach that treats the part of the breast where the tumor was removed after Breast conservation surgery (BCS). The number of fractions is increased per day, whiles the treatment area is decreased. This decreases the dose to normal tissue, resulting in less toxicity.

1.5.1 Patient Selection

When a patient is selected to receive APBI, a comprehensive evaluation must be performed to include patient and tumor characteristics as well as technical feasibility. All selection criteria must include patients who, first and foremost, are appropriate candidates for BCS [12].

A patient must also, meet the minimum requirements set by the recommendations of any of the following to receive APBI: the American Brachytherapy Society (ABS), the American Society of Breast Surgeons (ASBS), the American Society for Therapeutic Radiation Oncology (ASTRO), the National Surgical Adjuvant Breast and Bowel Project (NSABP) B-39/Radiation Therapy Oncology Group (RTOG)-0413, or the American College of Radiation Oncology (ACRO).

Table 3: Patient Selection Criteria for APBI.

Organization	Age (years)	Histology	Tumor size (cm)	Surgical Margins	LN Status
ABS [13]	≥ 50	All invasive subtypes and IDC	≤ 3	Negative	0
ASBS [14]	≥ 45	Invasive Carcinoma	≤ 3	Negative	0
	≥ 50	DCIS			
ASTRO [15]	≥ 50	Invasive ductal or DCIS	≤ 2.5	Negative	0
NSABP B-39/RTOG-0413 [16]	≥ 45	DCIS or Invasive Adenocarcinoma of the Breast	≤ 3	Negative	0-3
ACRO [17]	≥ 45	Invasive ductal carcinoma or DCIS	≤ 3	Negative	0

1.5.2 Fractionation: Prescription and Scheduling

Traditionally, the total dose typically prescribed is about 45-50 Grays (Gy) for the whole breast and/or lymph node areas. This is given once a day, 5 days a week for 5 to 7 weeks. The patient will receive 1.8-2 Gy per fraction. For APBI, the total dose is 34-38.5 Grays and the patient will receive about 3.4-3.85 Grays per fraction, twice a day for 5-7 days [18].

1.5.3 Rationale for APBI

The rationale for this approach is based upon the principle that higher doses of radiation are given to the tumor bed, to control small foci of cancer which, may be left

behind after surgery alone. Studies have shown, that more than 80-90% of local recurrences occur in the areas at or near the tumor bed [9] [12] [16] [19].

(Source: David E. Waver, Accelerated Partial Breast Irradiation)

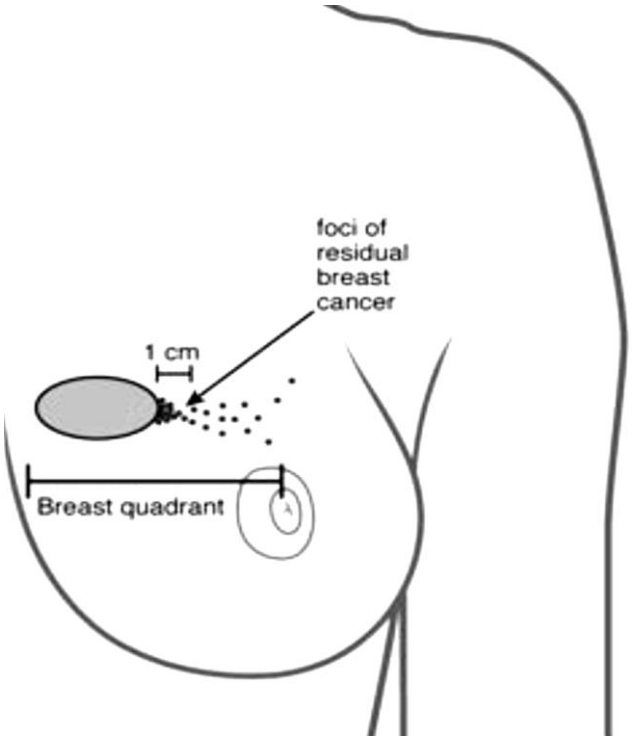

Figure 4: Illustration of a medial tumor bed with residual disease extending from the tumor bed into the upper lateral quadrant.

1.6 Most Commonly Used APBI Techniques

1.6.1 Three-Dimensional Conformal External Beam Radiotherapy

Three-dimensional conformal external beam radiotherapy (3D-CRT) is an external beam radiation therapy technique that is based on 3D anatomic information. A computed tomography (CT) scan is taking of the patient's breast before treatment to design a plan that conforms as closely as possible to the planned target volume using 3-5 field tangentially positioned non-coplanar beams.

1.6.2 Intraoperative Radiation Therapy

Intraoperative radiation therapy (IORT) is a new technique that allows the patient to receive radiation to the target during surgery. A single dose of 5-20 Gy is given directly to the exposed breast tissue using low x-ray or electrons. The main basis of IORT is that a single dose of IORT could have a biological effect on tissue that is equivalent to a full course of fractionated EBRT [12].

1.6.3 Multi-catheter Interstitial Brachytherapy

Multi-catheter interstitial brachytherapy (MIB) is a technique utilize radioactive source placed directly in the area where the cancer was. There are about 15-20 catheters placed throughout the breast tissues that surround the lumpectomy about 1 to 1.5 cm intervals. Using a remote afterloader, the radioactive source is placed inside the catheters for a few hour or days

1.6.4 Intracavitary Brachytherapy

Intracavitary brachytherapy is a technique that places a removable applicator (balloon-based or strut-based) in the lumpectomy cavity using a single opening in the skin. The applicator is expended for the duration of treatment and then removed at the end of treatment. This treatment also delivers the radiation source using a remote afterloader.

Mammosite Device

The Mammosite applicator is a silicone balloon filled with saline that is approximately 4-6 cm in diameter and surrounds a double-lumen catheter that is 15 cm long. The catheter has two channels. One channel inflates the balloon and the next channel allows the radioactive source to travel within the cavity.

(Source: Hologic: The Science of Sure)

Figure 5: Mammosite A) single-lumen, and B) multi-lumen balloon catheters.

Contura Multi-Lumen Device

The Contura applicator is similar to the Mammosite applicator. However, it offers 4 additional peripheral lumens. Each lumen is located 5 mm from the central lumen. These additional channels allow for a flexible dose distribution, which spares normal tissue.

(Source: Hologic: The Science of Sure)

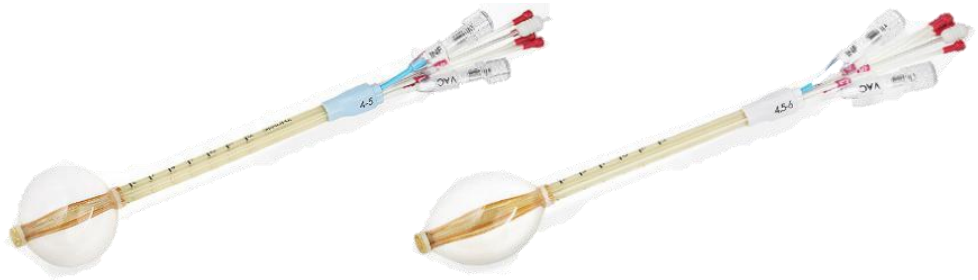

Figure 6: Contura multi-lumen balloon catheters in A) Circular and B) Elliptical.

Strut-Adjusted Volume Implant

The Strut-Adjusted Volume Implant (SAVI) applicator is a multi-catheter single entry device. It has a central catheter surrounded by additional peripheral struts. The device expands to fit the patient's lumpectomy cavity. Each catheter contains several dwell positions for the radiation source.

(Source: Cianna Medical)

Figure 7: SAVI applicator in multiple sizes.
6-1 mini, 6-1, 8-1, and 10-1 from top to bottom, respectively.

ClearPath

The ClearPath (CP) applicator is a similar to the SAVI 6-1 applicator. However, its radiation source is not in direct contact to breast tissue. ClearPath was developed to combine the advantage of balloon brachytherapy and multi-catheter brachytherapy.

(Source: North America Scientific)

Figure 8: ClearPath A) with base detached B) with a cap placed over the HDR channels.

1.7 B-39 Protocol Guidelines for Intracavitary APBI

1.7.1 Target Volumes

- Clinical Target Volume (CTV) – the area around the tumor or tumor bed that might have some microscopic disease.

- Planning Target Volume (PTV) – 1cm uniform expansion of the lumpectomy cavity volume.
- Planning Target Volume used for plan evaluation (PTV-eval) – Breast tissue volume bounded by the uniform expansion of the cavity's radius by 1cm in all dimensions minus the cavity's volume and is limited to 5 mm from the skin surface and by the posterior breast tissue extent [16].

1.7.2 Dose Volume Parameter

- For uninvolved normal tissue, it's ideal that less than 60% of the breast reference volume should receive at least 50% or more of the prescribed dose.
- For normal breast tissue that is receiving higher dose, the actual volume of tissue receiving 150% (V150) and 200% (V200) of the prescribed dose will be limited to ≤ 50 cc and ≤ 10 cc, respectively [16].

1.8 Brachytherapy Dose Calculations

Brachytherapy dose for a homogenous medium and point source are calculated according to the American Association of Physicists in Medicine (AAPM) Report No. 51 which is an update of the AAPM Task Group 43 (TG-43) recommendations.

1.8.1 General 2D formalism

The two-dimensional (2D) dose rate can be calculated according to the following:

$$\dot{D}(r,\theta) = S_K \cdot \Lambda \cdot \frac{G_L(r,\theta)}{G_L(r_0,\theta_0)} \cdot \ g_L(r) \cdot F(r,\theta)$$

Where,

r is the distance (cm) from the center of the active source to the point of interest,

r_0 is the reference distance which is specified to be 1 cm,

θ is the polar angle specifying the point of interest. $P(r,\theta)$, relative to the source longitudinal axis,

θ_0 is the reference angle, it defines the source transverse plane, and is specified to be 90° or π/2 radians.

S_K is the air-kerma strength.

Λ is the dose rate constant in water,

$G_L(r,\theta)$ is the geometry function,

$g_L(r)$ is the radial dose function, and

$F(r,\theta)$ is the 2D anisotropy function.

(Source: AAPM Report No. 51)

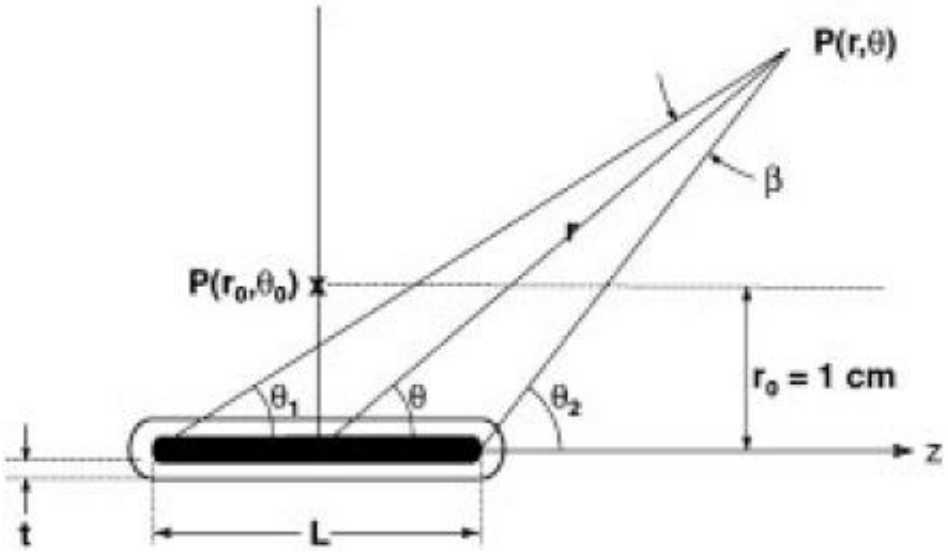

Figure 9: Coordinate system used for brachytherapy dosimetry calculations

The air-kerma strength is the air-kerma rate, $\dot{K}_\delta(d)$, in a vacuo and due to photons of energy greater than δ, at distance, d, multiple by the square of this distance, d^2, where d is the distance from the source center to the point of, $\dot{K}_\delta(d)$.

$$S_K = \dot{K}_\delta(d)d^2$$

The dose rate constant in water is the ratio of dose rate at the reference position $P(r_0, \theta_0)$, and S_K. The dose-rate constant depends on both the radionuclide and source model, and is influenced by both the source internal design and the experimental methodology used by the primary standard to realize S_K.

$$\Lambda = \frac{\dot{D}(r_0, \theta_0)}{S_K}$$

The purpose of the geometry function is to improve the accuracy with which dose rates can be estimated by interpolation from data tabulated at discrete points. It can be defined as the following:

For point-source approximation

$$G_P(r, \theta) = r^{-2}$$

For line-source approximation

$$G_L(r, \theta) = \begin{cases} \dfrac{\beta}{Lr\sin\theta} & if\ \theta \neq 0° \\ \left(r^2 - \dfrac{L^2}{4}\right)^{-1} & if\ \theta = 0° \end{cases}$$

Where,

B is the angle, in radians, subtended by the tips of the hypothetical line source with respect to the calculation point, $P(r, \theta)$.

The radial dose function accounts for dose fall-off on the transverse-plane due to photon scattering and attenuation and can be defined as the following:

$$g_X(r) = \frac{\dot{D}(r, \theta_0)}{\dot{D}(r_0, \theta_0)} \frac{G_X(r_0, \theta_0)}{G_X(r, \theta_0)}$$

The 2D anisotropy function by describes the variation in dose as a function of polar angle relative to the transverse plane and can be defined as the following [20]:

$$F(r,\theta) = \frac{\dot{D}(r,\theta)}{\dot{D}(r,\theta_0)} \frac{G_L(r,\theta_0)}{G_L(r,\theta)}$$

1.8.2 General 1D formalism

The one-dimensional (2D) dose rate can be calculated according to the following:

$$\dot{D}(r,\theta) = S_K \cdot \Lambda \cdot \frac{G_L(r,\theta_0)}{G_L(r_0,\theta_0)} \cdot \ g_L(r) \cdot \phi_{an}(r)$$

Where,

$\phi_{an}(r)$ is the 1D anisotropy function.

At a given radial distance, the 1D anisotropy function is the ratio of the solid angle weighted dose rate, averaged over the entire 4π steradian space, to the dose rate at the same distance r on the transverse plane and can be defined as the following [20]:

$$\phi_{an}(r) = \int_0^{\pi} \frac{\dot{D}(r,\theta)\sin(\theta)\,d\theta}{2\dot{D}(r,\theta_0)}$$

1.9 Clinical Process for Treating under B39 Protocol using a SAVI Applicator

1.9.1 Applicator Selection and Placement

As stated Section 1.6.4, the SAVI applicator is a multi-catheter single entry device that expands to fit the lumpectomy cavity of the patient, which is offered in multiple sizes. To determine the correct size for the patient, the medical doctor will evaluate the patient's cavity, after BCS, by measuring the long axis and diameter of cavity. Then a SAVI prep catheter (SPC) will be inserted into the cavity and filled with a saline base until a SAVI size resistance is achieved. The Conformance of SPC to cavity is verified using ultrasound and the measurements are compared to the size reference chart in Table 4 to determine which SAVI size is best suited for the patient. The Physician inserts the appropriate SAVI

in a closed position, and then expands the catheters to conform to the shape of the cavity. The ends of the catheters remain outside the breast for the entire treatment process [21].

Table 4: SAVI Size Reference Chart [21].

Long Axis	**Diameter of Cavity**		
	2-3 cm	**3-4 cm**	**4-5 cm**
2-3 cm	6-1 Mini	--	--
3-4 cm	6-1 Mini	6-1 Mini	--
4-5 cm	6-1 Mini	6-1 Mini	6-1
5-6 cm	6-1	6-1	8-1
6-7 cm	6-1	8-1	8-1
7-8 cm	8-1	10-1	10-1

1.9.2 Imaging

A Computed Tomography (CT) Scanner is used to take detailed x-ray images of the patient's structures. The patient is placed in a supine position on the couch of the CT scanner. Using immobilization devices, the patient's arms are placed above the head. Once the patient is ready for imaging, the patient will be aligned using the room lasers. The position of the setup is marked on the patient and recorded for reproducibility.

(Source: Cianna Medical)

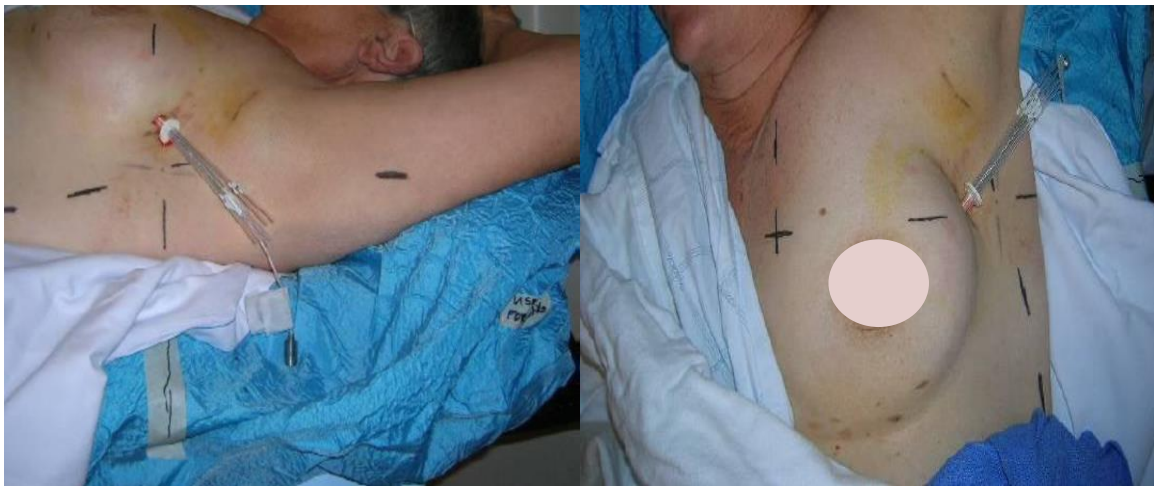

Figure 10: Example of patient setup including markings.

A scan of the whole breast is taken including AP and Lateral scouts. The CT should start at or above the mandible and extend several cm below the inframammary fold (including the entire lung). A CT scan thickness of ≤ 0.3 cm should be employed [16]. For better resolution, 1.0-2.0 mm slice thickness can be used. The images are saved and exported to the Treatment Planning System (TPS). The distance from skin to the hub (catheter handle) is measured and recorded. The length of each catheter is measured and recorded using a source position simulator.

1.9.3 Treatment Planning

Structure Definition

Structures of the following are created on the digital images: Lumpectomy cavity, Trapped air/fluid outside the applicator air, PTV, PTV-eval, Skin surface (5mm thickness), Chest wall and Ribs.

(Source: Edited screenshot from Oncentra TPS)

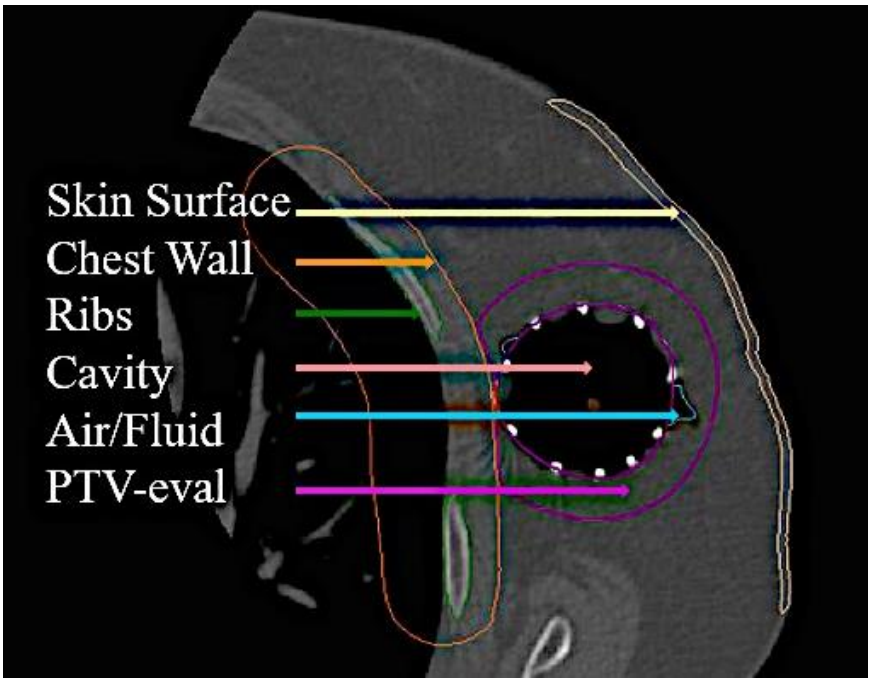

Figure 11: Planning CT scan with contoured structures.

Catheter Reconstruction

The catheters are reconstructed by rotating the axis in Extra Coordinate System (ECS), to view the SAVI from distal to proximal end. Strut 1 is in the center of the SAVI and struts 2, 4, and 6 can be identified by the markers at the top, middle, and bottom of the SAVI, respectively. Patient points can be used to label and further track the location of each strut. During catheter reconstruction, the number of catheters are added with only strut 1 having a 7.3 mm offset. Within each catheter, dwell times are selected at 0.5-cm intervals so that the PTV is covered by the prescription isodose line, with an acceptable dose homogeneity index [12].

(Source: Edited screenshot from Oncentra TPS)

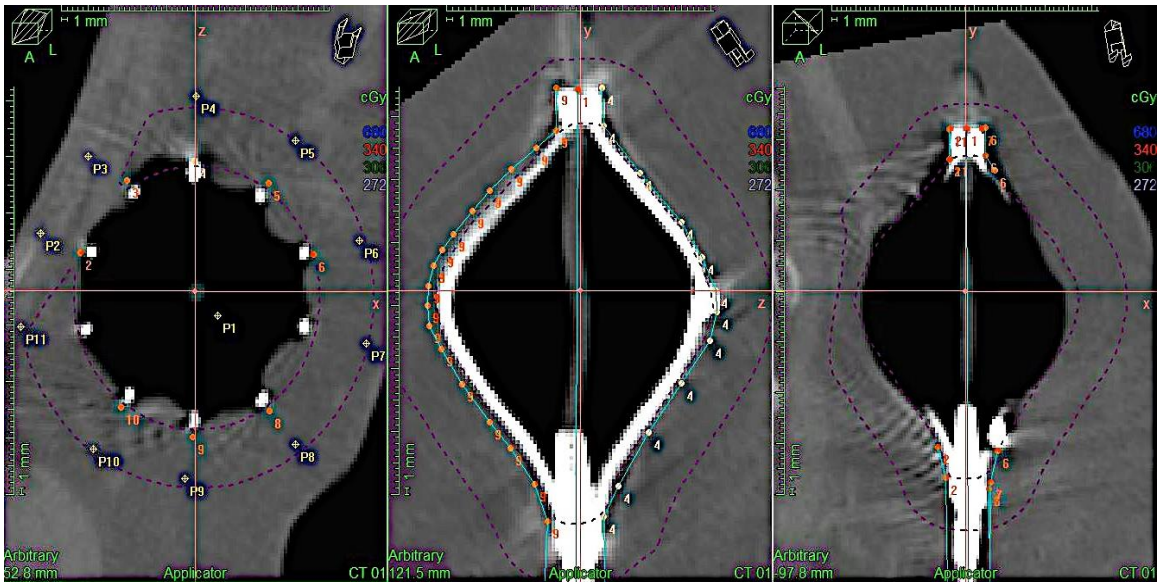

Figure 12: ECS view of the Catheters being reconstructed.

Catheter 4 (image B) and Catheter 6 (Image C) can be identify by their markers in the middle and bottom of the applicator, respectively.

Prescription

Once the catheter reconstruction is completed the prescribed dose can be inputted into the TPS. A total of 34 Gy will be delivered as per all dose requirements of target

coverage and dosimetric homogeneity. Two fractions per day, each of 3.4 Gy, separated by at least 6 hours, given over a period of 5 to 10 days.

Optimization

An optimized dose distribution is generated by an Inverse Planning Simulated Annealing (IPSA) algorithm. IPSA uses pre-desired maximum and minimum dose limits to the region of interest (ROI) set by the clinical objectives. A numerical weight value can be assigned to each ROI, with the higher weight number indicating the higher the level of importance.

1.9.4 Plan Evaluation

The treatment plan used for each patient will be based on analysis of the volumetric dose including dose-volume histogram (DVH) analyses of the planning target volume for evaluation (PTV-eval) and critical normal tissues [16].

1.9.4.1 DVH

The DVH is a graph that shows the volume of the ROI versus the dose distribution. There are two common formats of the DVH:

- The *cumulative* DVH is a plot of the volume of a given structure receiving a certain dose or higher as a function of dose.
- The *differential* DVH is a plot of volume receiving a dose within a specified dose interval as a function of dose.

1.9.4.2 Dosimetric Goals

- DVH analysis of target coverage will confirm ≥ 90% of the prescribed dose covering ≥ 90% of the PTV-eval.
- (% PTV-eval coverage) – [(vol trapped air/vol PTV-eval) x 100] ≥ 90%

- The volume of trapped air/fluid is < 10% of the PTV-eval.
- At least 95% of the Volume of PTV-eval (V95) is to receive 90% of the prescribed dose.
- Critical normal tissue DVHs within 5% specified value.
- The maximum skin dose at any point is ≤ 145% [16].

(Source: Edited screenshot from Oncentra TPS)

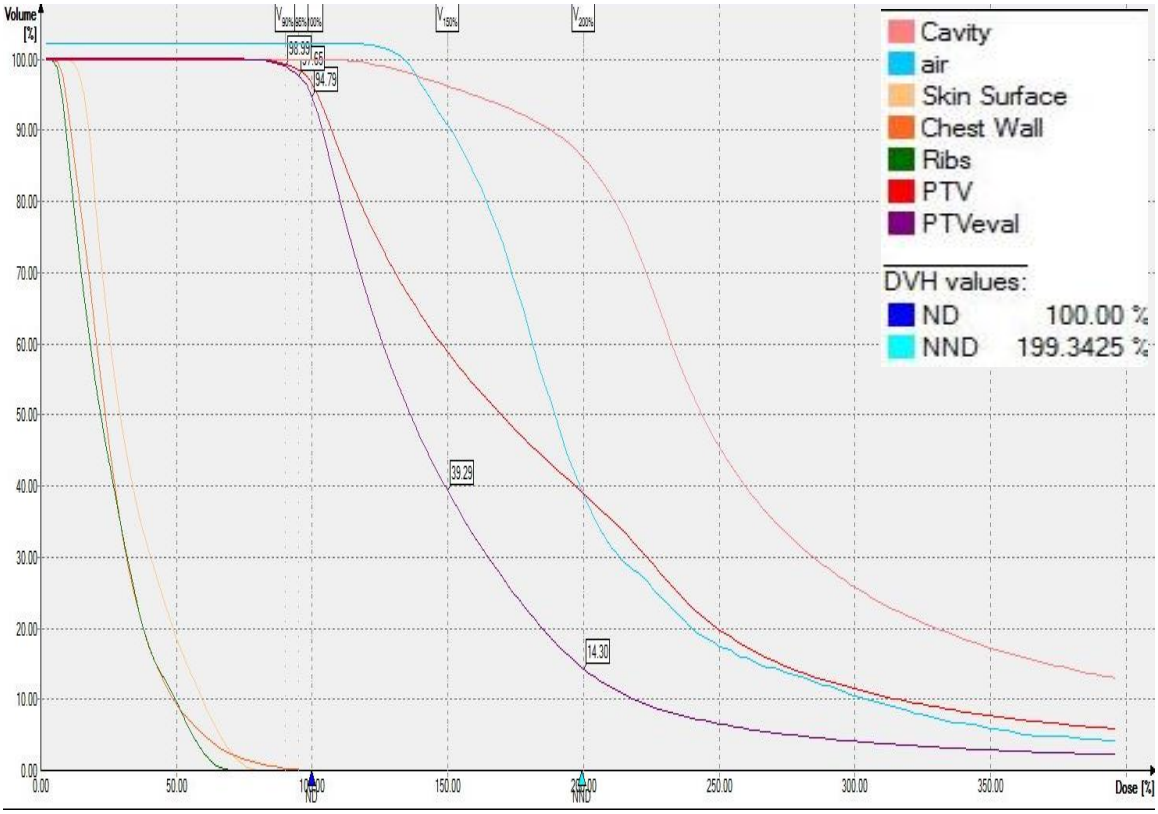

Figure 13: Cumulative DVH graph.

1.9.5 Delivering Treatment

CT Imaging and Device Verification

A CT scan must be taken prior to each fraction. The position setup must be identical as the first scan. AP and Later scouts and axial images are taken. The location of the SAVI must be evaluated. Any movement or rotation must be verified and recorded. The distance

from the applicator to the skin should be noted as well as any significant amounts of changes in air/fluid, to determine if a re-plan is necessary.

Preparing Afterloader

Each transfer tube should be connected to the afterloader by its identification number. The afterloader should be locked into place to secure the transfer tube.

Preparing Patient for Treatment

The catheter protectors are first removed and the expansion tool is inserted. The transfer guide tubes are securely connected to the afterloader using corresponding catheters. The transfer guide tubes should be extended for smooth travel of the radiation source. The patient is set up in the exact scanning position and is checked to ensure that there is no pulling of the application from the weight of the tubes.

Deliver Fraction

The patient's approved plan is imported into the Treatment Delivery Console. A Quality Assurance (QA) check is ran prior to delivering the fraction to compare and verify the coordinates and dwell times against the treatment plan printout. The Medical Physicist and Physician must be present during the entire fraction delivery. During treatment, the radiation source, Iridium 192 (Ir-192) connected to a stainless-steel cable, is transferred from the afterloader's lead housing to different position in the patient via the transfer tubes and kept for a few seconds according to the need to deliver the desired dose. The source is retracted back into the afterloader once the treatment delivery is completed.

1.10 Thermoluminescent Dosimetry

Luminescence is the emission of light from a material following the initial absorption of energy from an external source. The emission can be categorized as either

fluorescence or phosphorescence [22]. The difference of them is the time delay between the stimulation and the emission of light. Fluorescence has a time delay of 10-10 – 10-8 s, and phosphorescence has a time delay exceeding 10-8 s.

Thermoluminescent (TL) means is a form of luminescence in which light is emitted after a material is heated. The two most common types of materials that exhibit thermoluminescent in response to ionizing radiation are calcium fluoride (CaF_2), and lithium fluoride (LiF.)

1.10.1 Thermoluminescent Dosimeters

A thermoluminescent dosimeter (TLD) is a type of radiation dosimeter that measures ionizing radiation exposure by measuring the intensity of visible light emitted from a crystal in the detector when the crystal is heated [23]. TLD was invented in 1954 by Professor Farrington Daniels of the University of Wisconsin-Madison [24].

Today, TLDs are mostly used in applications of dosimetry for in-phantom and in-vivo dosimetry. As well as, in radiation protection for personal monitoring of radiation workers. The TLDs most commonly used materials in medical applications are LiF:Mg,Ti, LiF:Mg,Cu,P and Li_2B4O_7:Mn, because of their tissue equivalence. Other TLDs, used because of their high sensitivity, are $CaSO_4$:Dy, Al_2O_3:C and CaF_2:Mn.

1.10.2 TLD Theory

TLD relies on the fact that, in certain imperfect crystals, electrons are trapped in metastable states. When energy is absorbed from incident radiation, electrons are raised from the valence to the conduction band. Some of the electrons return instantly to the valence band, but others are "trapped" in intermediate energy levels supplied by impurities in the crystals. The number of trapped electrons is proportional to the energy

absorbed from the radiation. Unless energy is supplied to the crystals, most of the trapped electrons remain in the intermediate energy levels for an indefinite period.

(Source: Emma Viviers, Medical Physics Diagrams)

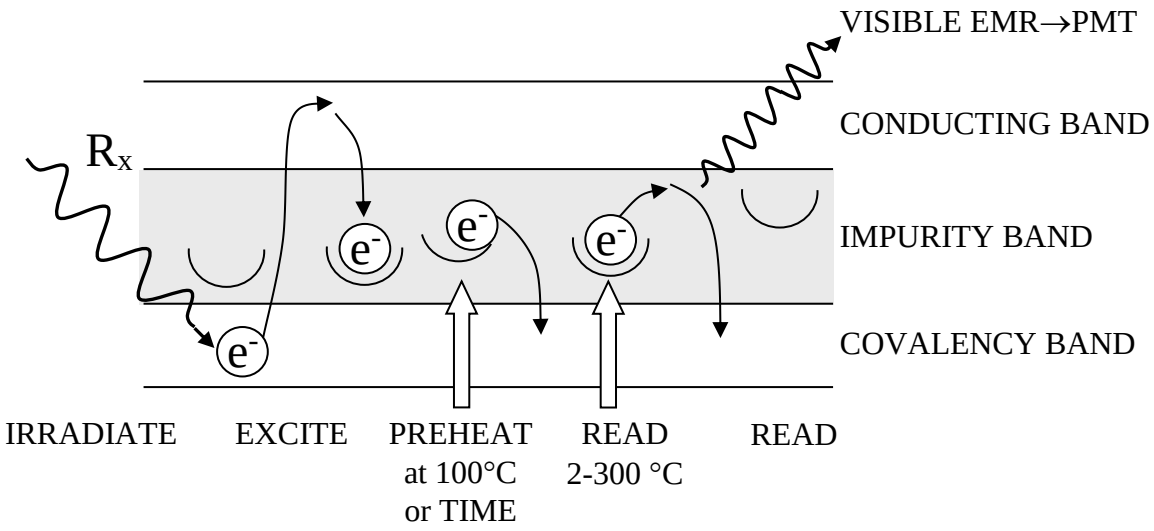

Figure 14: Schematic diagram of the TLD process.

If the crystals are heated, however, the trapped electrons are released and return to the conduction band. These electrons then fall to the valence band, releasing light in the process. The light is directed onto a point to generate an electrical signal proportional to the energy originally deposited in the crystals by the radiation. Detection of this signal yields a measure of the absorbed dose in the crystals [25].

1.10.3 The Reading System

A basic TLD reader system consists of:

- A *planchet* heated by an electric current, which is used for placing and heating the TLD,

- A *photomultiplicator tube* (PMT), which is used to detect the TL emission and convert it into an electrical signal linearly proportional to the detected photon fluence, and
- An *electrometer*, for recording the PMT signal as a charge or current.

(Source: Philip Mayles, Handbook of Radiotherapy Physics)

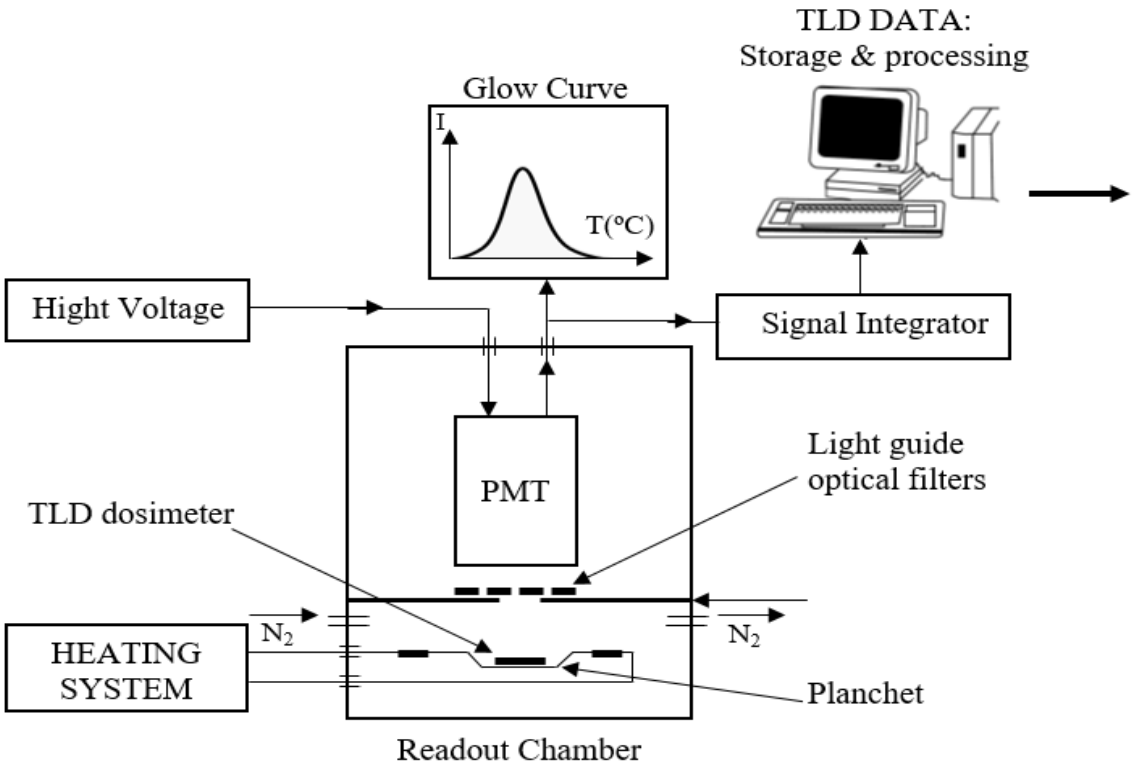

Figure 15: Schematic representation of a TLD Reader.

The TLD Reader shown in the above figure contains a heating system housed in a readout chamber, a light detection system, a signal integrator, and a PC and Associated Software [26].

1.10.4 Time Temperature Profile

Because the response of the TLD material is affected by their pervious radiation history and thermal history, the material must be suitably annealed to remove residual

effects [27]. A time temperature profile (TTP) is the temperature to which the TLD material is heated as a function of time. It is defined in three segments:

- Preheat establishes a common starting point for all dosimeters in a group and may be used to eliminate the faster-fading low temperature peaks.
- Acquisition is the segment during which the dosimetric data is acquired and the glow curve is generated.
- The anneal segment is used to hold the dosimeter at a high temperature to ensure that the entire TL signal is removed [28].

(Source: Emma Viviers, Medical Physics Diagrams)

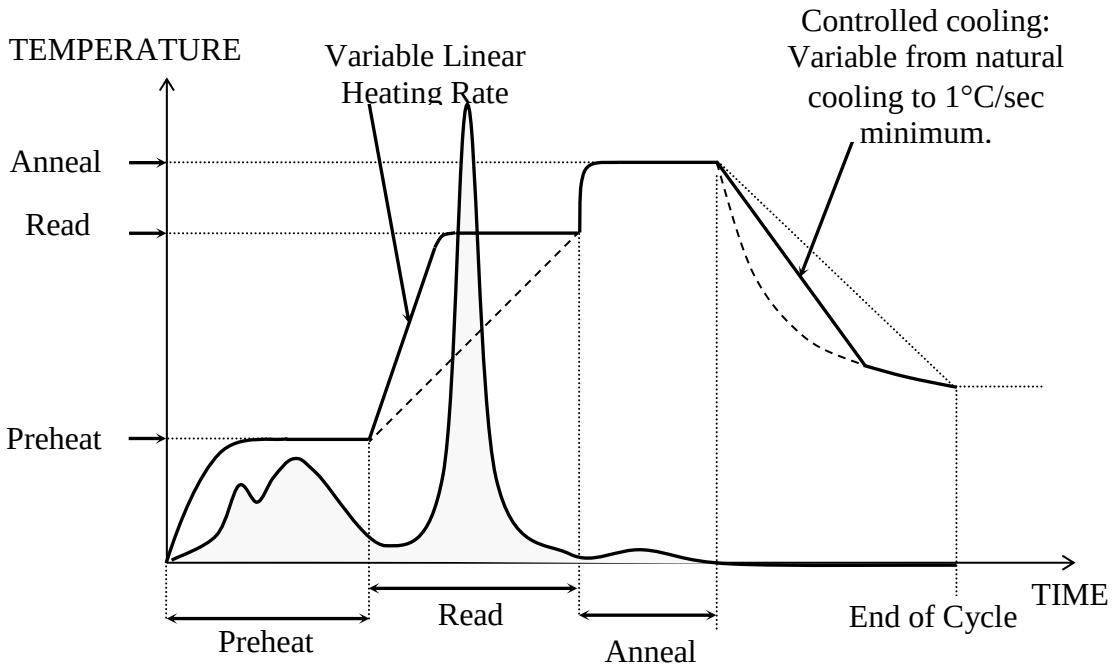

Figure 16: Typical TTP and glow curve for LiF: Mg,Ti exposed to 1 Gy.

1.10.5 Glow Curve

The glow curve is a plot of the TL intensity, I, as a function of the TLD temperature, T, during read out. As the temperature of the TL material exposed to radiation is increased, the probability of releasing trapped electrons increases. Each

trapping level in the material gives rise to an associate glow peak. Keeping the heating rate constant makes the temperature T proportional to time t and so the TL intensity can be plotted as a function of t [27] [28] [29].

1.10.6 Reader Calibration Factor

The Reader Calibration Factor (RCF) is the factor that converts the raw charge data in nanocoulombs (nC) to dosimetric units or generic units for input to an algorithm.

$$RCF = \frac{< Q >}{L}$$

Where,

<Q> is the mean charge of a set of Calibration Dosimeters.

L is a known quantity of radiation L.

The value of the RCF provides the main link between the TL response in terms of charge or counts (C) and the absorbed dose in Gray (Gy) or dose equivalent in Sievert (Sv) [28].

1.10.7 Element Correction Coefficient

The Element Correction Coefficient (ECC) is the calibration factor for TLDs. The ECC is used as a multiplier with the Reader output (nC) to make the response of each dosimeter comparable to the average response of a designated group of dosimeters maintained as calibration dosimeters.

$$ECC_i = \frac{< TLE >}{TLE_i}$$

Where,

TL efficiency (TLE) is defined as the emitted TL light intensity per unit of absorbed dose [28].

1.10.8 Dose Calculation

To derive the absorbed dose from the TL-reading after calibration, correction factors must be applied: energy correction, fading, dose response non-linearity corrections. The algorithm which can be used to convert the light emission obtained during the readout of a thermoluminescent detector to the absorbed dose can be expressed by the following relationship, which includes all the parameters which can influence the dose:

$$D = M_{net} * S_i * F_C * F_{st} * F_{en} * F_{lin} * F_{fad}$$

Where,

M_{net} is the net TL signal,

S_i is the relative intrinsic sensitivity factor,

F_C is the individual calibration factor of the detector,

F_{st} is the factor which considers the possible variations of F_C due to variations of the whole dosimetric system and of the experimental conditions,

F_{en} is the factor which allows for a correction for the beam quality,

F_{lin} is the factor which considers for the non-linearity of the TL signal as a function of the dose, and

F_{fad} is the correction factor for fading [28] [29].

2. METHODS AND MATERIALS

2.1 Procedure

A set of CT images were selected from a patient who received APBI using the SAVI applicator. The patient's CT images were sent to .decimal, Inc (dot decimal) and 3D models made of tissue equivalent wax were printed. TLDs were calibrated for Brachytherapy before and after this study.

The 3D models were shaved to fit the expanded SAVI 10+1 applicator. Various points of interest were marked out and 1mmx2mm slots were carved in the phantoms to fit the dummies and then the TLD chips. CT scans were taken of the 3D model with SAVI applicator inserted and the dummies placed over the slots.

The images were imported into Oncentra TPS and a plan was made following B-39 protocol. The plan was exported to treatment console. The dummies were replaced with the TLDs, and they were expose during treatment delivery. The TLD were read and the absorbed doses were calculated and compared to the delivered dose.

2.2 Phantom Modeling

One breast cancer case was selected to be the modeled for this study.

2.2.1 Three-Dimensional (3D) Printing

Three-dimensional (3D) printing is a manufacturing method in which objects are made by fusing or depositing materials—such as plastic, metal, ceramics, powders, liquids, or even living cells—in layers to produce a 3D object. This process is also referred to as additive manufacturing (AM), rapid prototyping (RP), or solid free-form technology (SFF).

2.2.2 Printing Process

The printing process consists of a basic setup. A shape is defined in a computer-aided design (CAD) file. The 3D printer first follows the instructions in the CAD file to build the foundation for the object, moving the printer head along the x-y plane. Then the printer continues to follow the instructions, moving the printer head along the z-axis to build the object vertically, layer by layer.

Using the original CT images of the patient, structures were outlined for printing and uploaded to .decimal, Inc. and a uniform 3D phantom made of Deep Blue Wax. This wax is a non-hazardous material known as a Proprietary mixture.

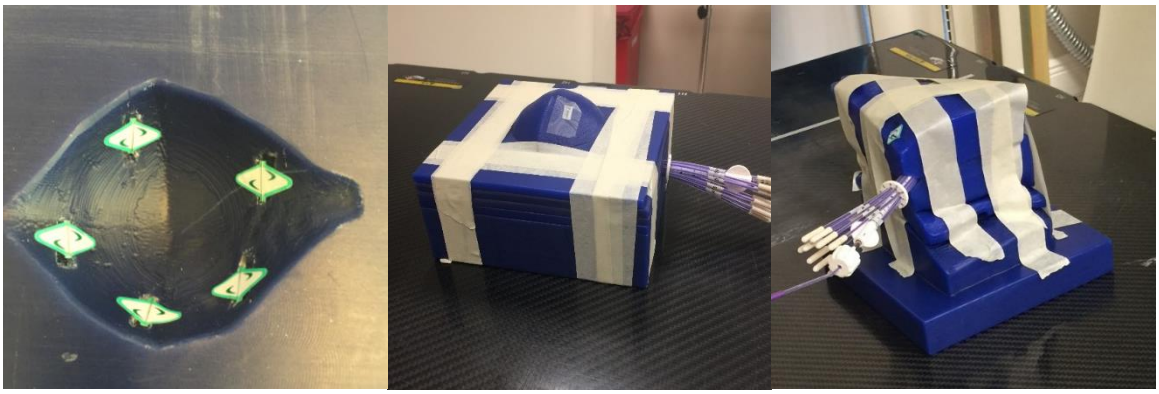

Figure 17: A) Surface of the cavity in the tissue with dummies placed. B&C) 2 sets of 3D printed structures ready to be scanned.

2.3 Planning on the Phantom

CT scan were taken with a slice thickness of 1.5 mm. The images were imported to Oncentra TPS and structures of the following – Cavity, PTV, PTV-eval, Skin Surface, Chest Wall, and Ribs were contoured for each phantom, along with TLD structures using the markers as reference locations.

(Source: Edited screenshot from Oncentra TPS)

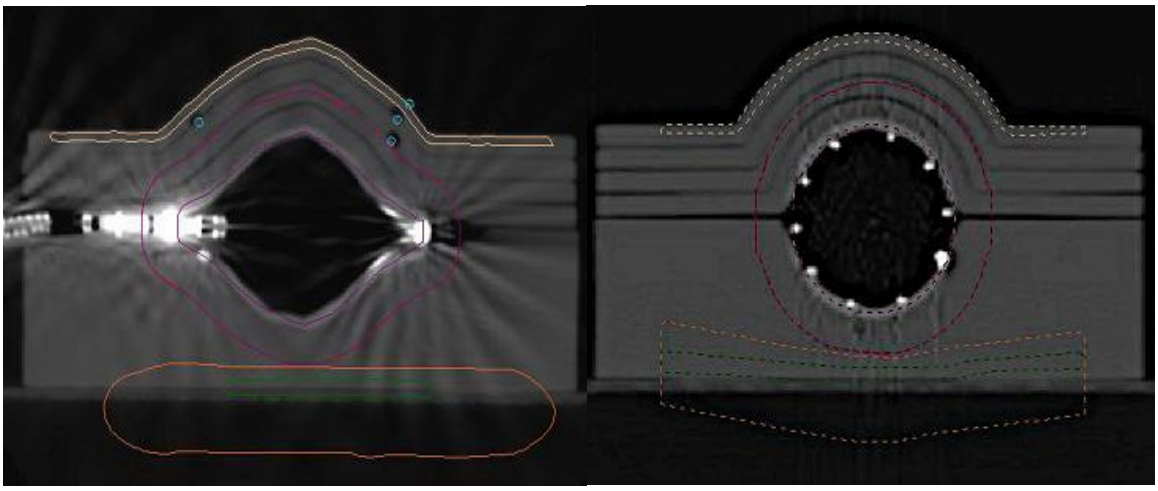

Figure 18: CT images of the 3D prints and the reconstructed structures on test 1.

(Source: Edited screenshot from Oncentra TPS)

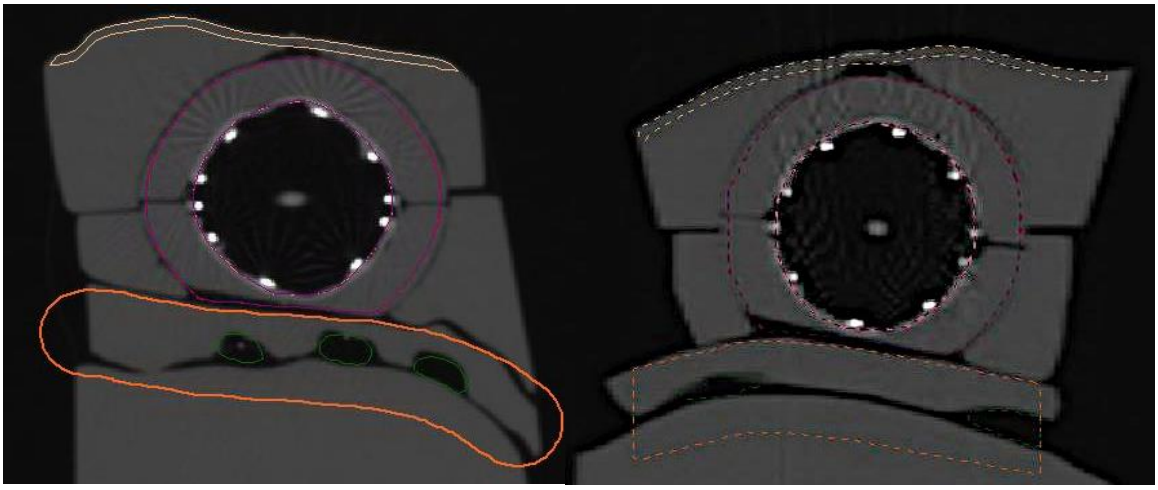

Figure 19: CT images of the 3D prints and the reconstructed structures on test 2.

2.4 Data Collection

After creating structures for the TLD markers, points were placed in the center of each structure to collect the absolute point dose computed by the TPS.

(Source: Edited screenshot from Oncentra TPS)

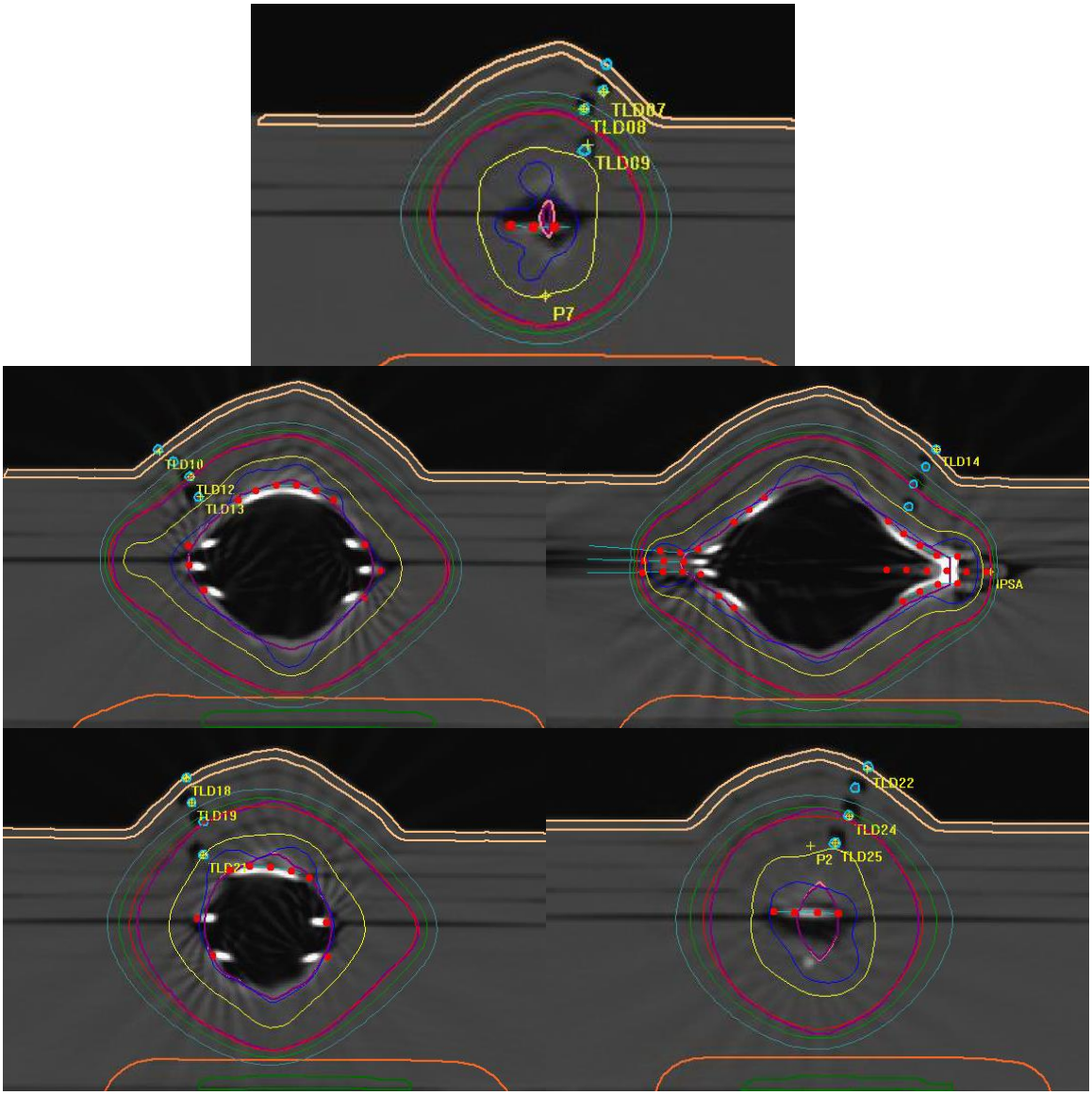

Figure 20: Various Points marked for dose collection on test 1.

(Source: Edited screenshot from Oncentra TPS)

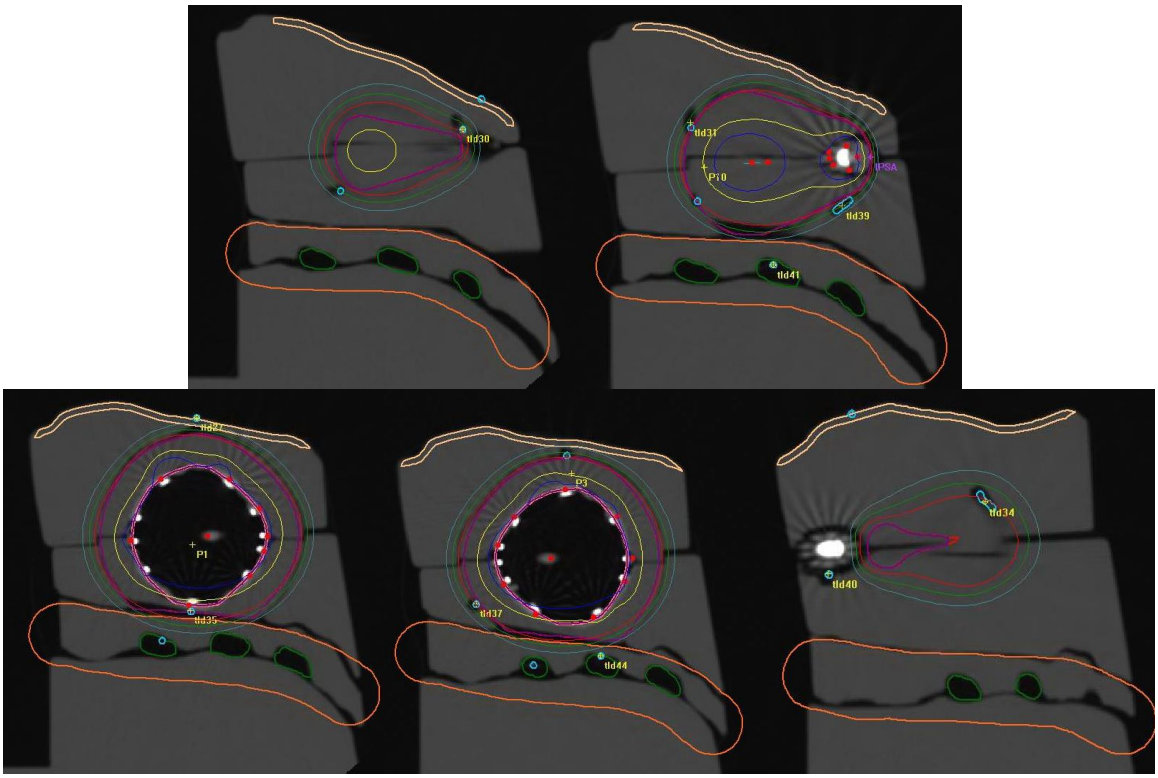

Figure 21: Various Points marked for dose collection on test 2.

(Source: Edited screenshot from Oncentra TPS)

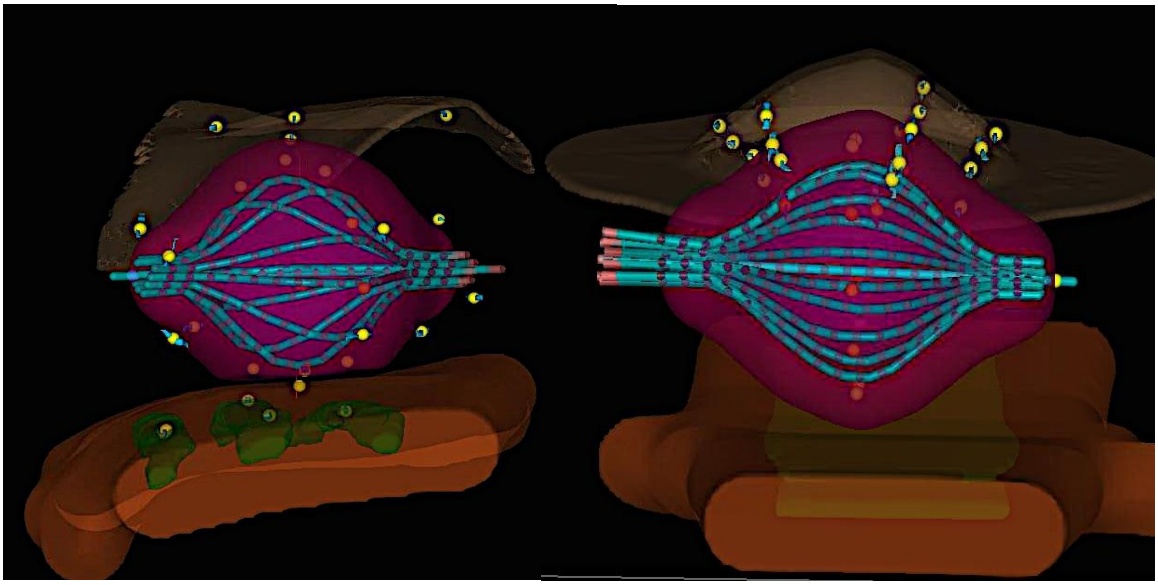

Figure 22: A 3D look of the Various TLD points marked for dose collection.

2.5 Irradiation

After the scan, the dummies were replaced with the TLD detectors. The treatment plan was imported to the treatment console and the treatment was delivered to each phantom.

Figure 23: Left) Phantom with the SAVI and TLDs in place. Right) Phantom connected to the afterloader, ready to be irradiated.

2.6 TLDs

Lithium fluoride with 2 impurities injected, Magnesium and Titanium (LiF:MgTi) is most commonly known as TLD-100. It was selected for this study because of several properties, such as tissue equivalence, relative low fading, and sensitivity.

2.6.1 Annealing

For the annealing procedure, the TLDs are placed on trays of stainless steel and annealed for 1 hour at 400 °C in an oven followed by fast cooling down to room temperature. This is followed by 2 hours annealing at 100 °C to reduce low-temperature peaks and final cooling down.

2.6.2 TLD Batch Sorting and Calibration

An Exposure Report and Calibration Report is printed out which includes: the date, time, TTP, Dosimeter ID, and ECC for each TLD. There were 4 batches of TLDs. Each batch containing 49 TLDs. The TLDs that varied more than ±2.5% from the median exposure value were excluded from sorting. Then the TLDs with similar ECC values were paired together. A minimum of 11 pairs were made for each batch. The lowest and the highest pairs were keep aside for calibration control. The controls were then irradiated and the correction factor for the beam quality was determined for each batch.

2.6.3 Ir-192 Calibration

In efforts to ensure the most accurate results, a set of 5 TLDs were calibrated before the start of the process and another set of 5 at the end. Using 2 cured transparent gel encased in a layer of polyurethane skin (Bolus) and 1 catheter, 200cGy was delivered to TLDs from each batch.

2.6.4 Read-out

After irradiation, the TLDs were read using a Harashaw TLD Model 5500 Automatic Reader Machine. Before the readout a pre-heat at 100 °C for 10 minutes was applied. An Exposure Report was generated which included the date, time, dosimeter ID, and a reading (Gy) for each TLD.

3. CALCULATIONS

3.1 Method for Calculating the Calibrated TLDs for HDR

To get the post-irradiation ECC, the pre-irradiation ECC was multiplied by the average ECC of the reference TLD used for calibration, for each batch. Next, the superlinearity (SL) was determined from the Table 5 based on the expected dose.

Table 5: Superlinearity Chart.

SL	Dose (cGy)
1.00	1-100
1.02	101-150
1.03	151-210
1.04	211-265
1.05	266+

The measured dose was calculated by multiplying the reading (cGy) by the ECC and divided by the SL, as shown in the following equation. The highest reading of the pairs was then recorded and compared to the expected dose.

$$Dose(cGy) = \frac{Measured\ Dose(Gy) * ECC}{SL}$$

3.2 Method for Calculating the Measured Dose from the Readings

The same method was used to calculated the measured dose; however, the raw reading was multiple by the HDR correction factor ($CF_{Ir\text{-}192}$) determined by the pervious result from the HDR calibration. The pre-irradiation ECC was multiplied by the average

ECC of the reference TLD used for calibration, for each batch. The superlinearity (SL) was determined from the Table 5 based on the expected dose. The measured dose was calculated by multiplying the raw reading (cGy) by the ECC and divided by the SL. The average reading of the pairs was then recorded and compared to the expected dose.

$$Dose(cGy) = \frac{Measured\ Dose(Gy) * CF_{Ir-192} * ECC}{SL}$$

Table 6: Sample Lab Data Calculations Sheet for TLD AV 01/04.

TLD ID	Readings (cGy)	ECC	SL	Dose (cGy)	Average/Highest Reading	Expected Dose (cGy)	% Diff
1	1795	1.11	1.03	193.4	--	192.8	--
4	1761	1.12	1.03	191.5			

3.3 Method for Calculating the Percentage Difference

The absolute percentage difference was calculated by subtracting the measured dose from the expected dose, then dividing the value by the expected dose, as shown in the following equation.

$$\%\ Diff = \left|\frac{Expected\ Dose - Measured\ Dose}{Expected\ Dose} * 100\%\right|$$

4. RESULTS AND DISCUSSION

4.1 Results from Measuring Dose at 0.5cm Increments

Table 7 shows the absolute percentage difference from Test 1 of measuring the dose at various point in 0.5cm increments from the PTV. All of the results from this test show that the measurements where within 10% tolerance limits, except 1. At 2.0 cm from the PTV, the result showed the highest deviations, with 11.51% being the highest.

Table 7: Result from measuring dose at 0.5cm increments.

Increments (cm)	TLD Pair ID	TLD 1	TLD 2	Average Reading (cGy)	Calculated Dose (cGy)	Absolute % Difference
2.0	6	155.11	154.24	154.68	174.80	11.51
	10	196.35	194.78	195.57	206.15	5.13
	14	175.47	178.28	176.88	191.51	7.64
	18	170.24	171.35	170.80	189.60	9.92
	22	168.90	163.50	166.20	181.74	8.55
1.5	7	210.42	224.74	217.58	226.31	3.86
	11	244.60	259.90	252.25	264.15	4.51
	15	235.34	238.43	236.89	242.89	2.47
	19	224.73	227.26	226.00	248.28	8.98
	23	232.65	227.90	230.28	235.33	2.15
1.0	8	294.90	292.14	293.52	293.17	0.12
	12	335.23	340.50	337.87	341.36	1.02
	16	326.80	323.10	324.95	319.96	1.56
	20	318.78	317.78	318.28	326.30	2.46
	24	292.73	290.20	291.47	315.77	7.70
0.5	9	453.80	429.30	441.55	439.04	0.57
	13	516.60	506.42	511.51	482.01	6.12
	17	474.91	478.07	476.49	464.68	2.54
	21	490.60	488.70	489.65	506.30	3.29
	25	453.02	439.64	446.33	467.92	4.61

4.2 Results from Measuring Dose at near Critical Structures

Table 8 shows the absolute percentage difference from Test 2 of measuring the dose at various point near critical structures. Each structure had variations above and below 10% of tolerance limit. The distal end of the SAVI applicator reflected the greatest deviations of 48.02%. The rib followed at 22.14%, then the skin surface at 17.57%, the PTV at 17.76% and the proximal end of the SAVI at 16.84%.

Table 8: Results from measuring dose near critical structures.

Structure	TLD Pair ID	TLD 1	TLD 2	Average Reading (cGy)	Calculated Dose (cGy)	Absolute % Difference
Skin Surface	26	137.99	156.56	147.28	172.96	14.85
	27	239.50	226.05	232.78	241.89	3.77
	28	148.10	142.20	145.15	176.09	17.57
	29	89.04	89.87	89.46	97.01	7.79
PTV	31	322.97	319.78	321.38	336.00	4.35
	32	297.10	327.96	312.53	337.59	7.42
	33	346.40	377.90	362.15	324.67	11.54
	34	372.31	377.00	374.66	345.63	8.40
	35	465.50	452.10	458.80	405.31	13.20
	36	375.30	372.30	373.80	332.41	12.45
	37	343.05	341.72	342.39	290.74	17.76
	38	273.01	271.54	272.28	318.93	14.63
	39	323.40	324.90	324.15	319.76	1.37
Ribs	41	225.30	243.19	234.25	191.78	22.14
	42	134.14	126.49	130.32	132.73	1.82
	43	246.15	236.65	241.40	216.98	11.25
	44	239.01	231.02	235.02	235.88	0.37
Proximal SAVI Tip	30	284.10	263.90	274.00	329.47	16.84
Distal SAVI End	40	263.36	231.81	247.59	167.27	48.02

4.3 Superficial Doses vs Deep Doses

The results from Table 7 showed that the doses at 2.0cm away from the applicator had higher variance compared to the doses at 0.5cm away. On average, the doses increased

at about 9% higher than the calculated TPS dose at 2.0cm, whiles the dose varied around 3-4% at locations closer to the PTV.

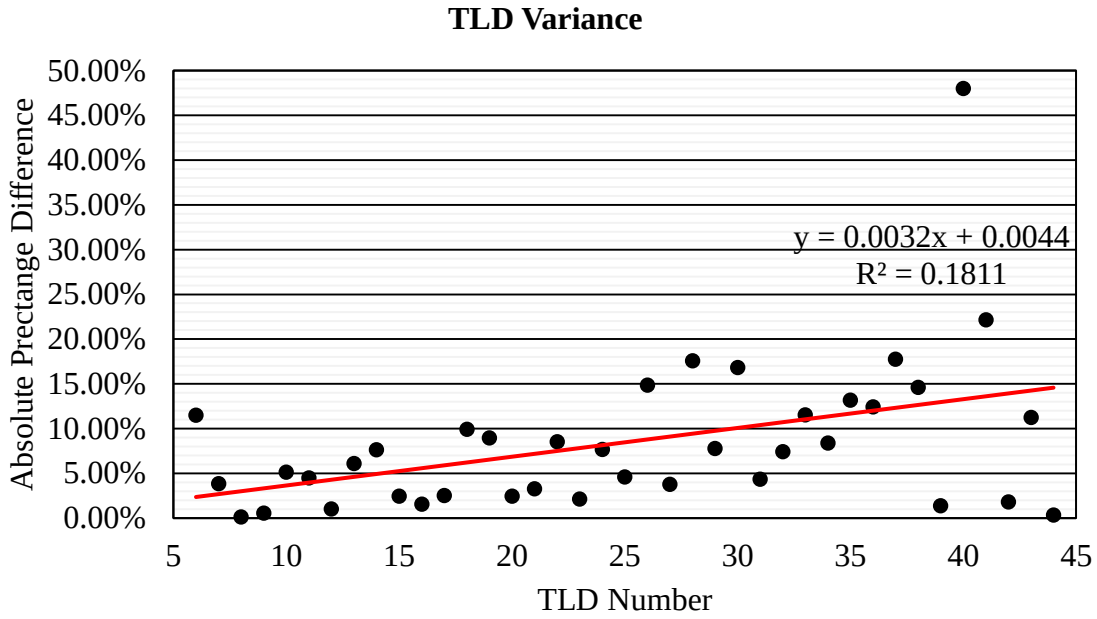

Figure 24: Plot of the linear fit of the variance of absolute percentage difference of each TLD.

4.4 Dose Overestimates by TPS

These results coincide with a study done by Julie Raffi of the University of Wisconsin-Madison, who quantify the TPS overestimation of the exit skin dose for a group of patients and several phantom configurations, concluded with results of an overestimated exit skin dose calculations by the TPS [30]. Another study done by Susan Richardson of Washington University School of Medicine who investigated the discrepancy between homogeneous dose calculations compared with heterogeneous calculations, resulting in overestimated doses in all evaluated regions [31]. As well as Melissa Lamberto of Christiana Care Health System, where TG-186 dose calculations were compared to TG-43. The results showed that TG-43 had higher skin dose values compare to TG-186 [32]. The

results of this study have concurred with those studies showing all TLDs placed on the skin surface were under estimated by an average of 11%.

4.5 Variations Due to Air

According to a study done by Scott Sample of Cancer Treatment and Cancer Care with Texas Oncology, who analyzed the dose enhancements of the TPS due to air in cavity of the SAVI, concluded that the dose in air had higher variance (13%) compare to dose in tissue (9%) and water (1%) [33]. Another study done by Susan Richardson of Washington University School of Medicine, who investigated the dosimetric effect of the air inside the SAVI, resulted in a 3-9% range of dosimetric effects of the air cavity. It is believed that the results from this study are statistically higher due to the air in the slot created in the phantoms to hold the TLDs, as well as the air in between the phantom sections. It is also believed that the results would significantly differ if this study was repeated in water.

4.6 Variation Due to Errors

Due to the random variation in the results (shown in the Figure 24), it is believed that several factors could have occurred such as:

- The TLD's virtual location in the TPS vs actual location in phantom,
- Set-up errors,
- Shifts in the TLDs' position after placement on the phantom,
- Fading between time of irradiation to the time of reading the TLDs, or
- Uncertainties in the TLD material.

5. CONCLUSION

The results of this study show that the overall average reading of the TLDs is within the expected value of 10%. The TPS shows overestimated dose calculations for brachytherapy. The calculated dose from the TPS for APBI brachytherapy treated with a SAVI applicator should be assess to account for the inhomogeneities. In the future, this study can be reconsidered to include heterogeneity corrections, in water conditions, and the TLD locations and proximity, as well.

APPENDICES

Appendix A: TLD Sorting and Calibration Report Summary

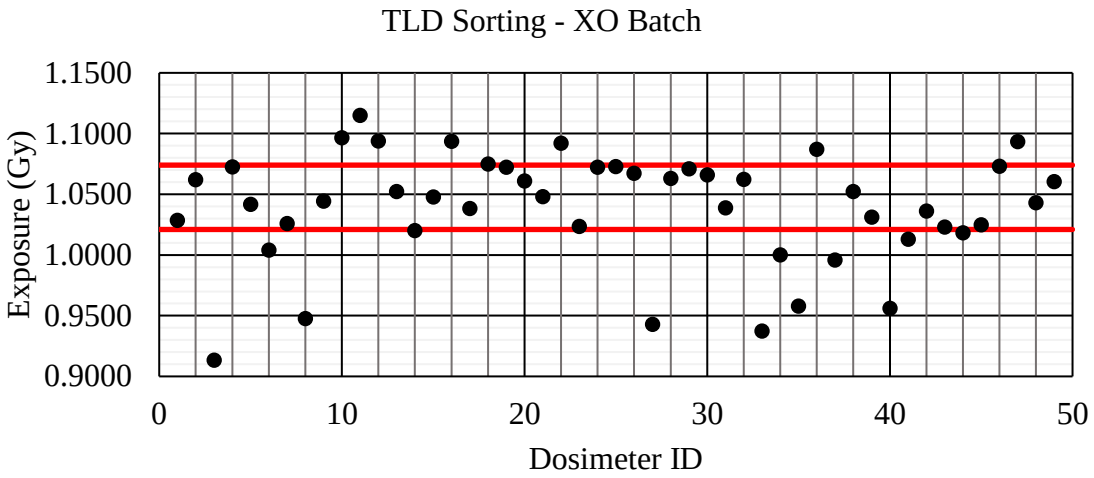

Figure 25: TLDs reading versus the number of TLDs for XO Batch.

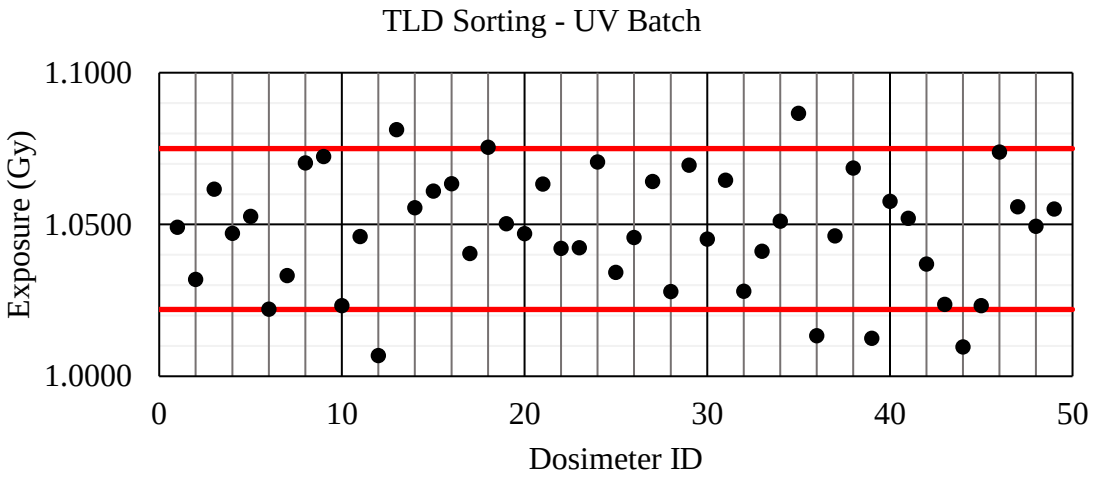

Figure 26: TLDs reading versus the number of TLDs for UV Batch.

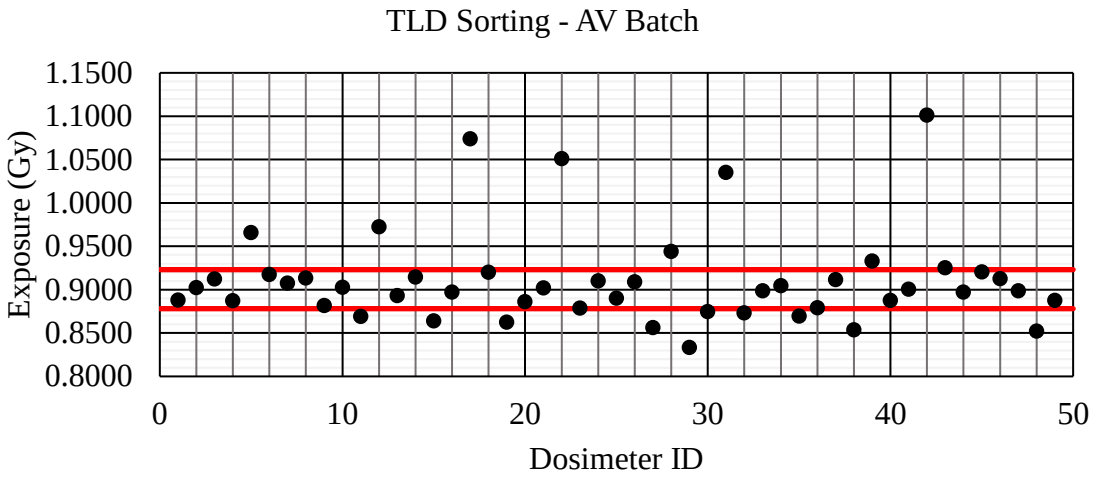

Figure 27: TLDs reading versus the number of TLDs for AV Batch.

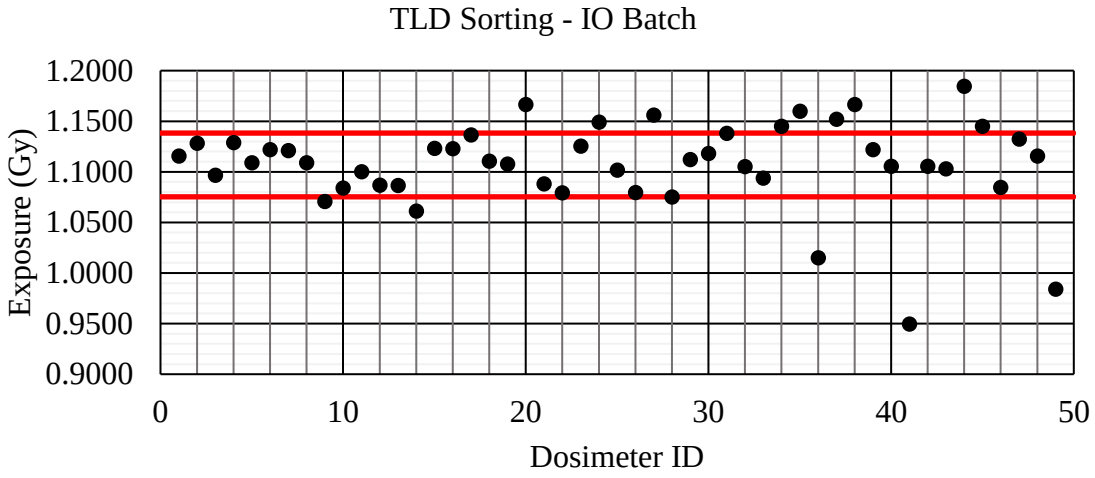

Figure 28: TLDs reading versus the number of TLDs for IO Batch.

Table 9: TLD Calibration Report summary.

Batch ID	Number of TLDs	ECC upper Value	ECC lower value	PMT Noise (nC)	Reference Light (nC)	RCF	Number of Pairs	F_{en}
XO	49	1.01	0.99	0.0048	5.590	43.36	12	1.02
UV	49	1.01	0.99	0.0049	5.559	43.36	17	1.00
AV	49	1.01	0.99	0.0051	5.617	43.36	13	0.99
IO	49	1.01	0.99	0.0050	5.559	43.36	15	1.01

Appendix B: TLD Post Irradiation Exposure Report

Table 10: Post – Irradiation Exposure Report for Batch XO.

TLD Pair ID	TLD ID	Reading (Gy)	TLD ID	Reading (Gy)
Control 1	2	1.9648	32	1.8925
Control B	28	2.2989	30	2.1155
17	4	5.2962	19	5.3303
8	5	3.1942	31	3.1551
20	9	3.4618	48	3.4406
23	13	2.5451	38	2.4454
10	15	2.0980	21	2.0823
26	20	1.4931	49	1.7263
32	24	3.3119	25	3.6582
36	26	4.1641	29	4.1452

Table 11: Post – Irradiation Exposure Report for Batch UV.

TLD Pair ID	TLD ID	Reading (Gy)	TLD ID	Reading (Gy)
Control 3	1	1.9935	48	1.9321
Control 5	2	1.6848	7	1.7545
Control D	40	2.0674	49	2.2699
Control A	43	2.0166	45	1.8430
21	3	5.3841	15	5.3607
9	4	4.9130	20	4.6473
16	5	3.5977	41	3.5143
11	11	2.6206	26	2.7828
22	14	1.8076	47	1.7506
28	17	1.5631	33	1.5018
30	19	3.0850	34	2.8684
33	22	3.7323	23	4.0725
35	25	4.9774	42	4.8471
39	28	3.437	32	3.4535
41	30	2.3892	37	2.5806

Table 12: Post – Irradiation Exposure Report for Batch AV.

TLD Pair ID	TLD ID	Reading (Gy)	TLD ID	Reading (Gy)
Control 2	1	1.7952	4	1.7608
Control E	46	1.7951	47	1.6609
25	2	4.3712	10	4.2421
12	7	3.2524	26	3.3094
7	9	1.9649	36	1.9708
19	13	2.1267	16	2.1602
14	20	1.6314	40	1.6605
27	21	2.2895	34	2.1662
31	24	3.1447	37	3.1165
40	25	2.4660	33	2.0165
44	41	2.2801	44	2.1960

Table 13: Post – Irradiation Exposure Report for Batch IO.

TLD Pair ID	TLD ID	Reading (Gy)	TLD ID	Reading (Gy)
Control 4	1	2.0898	48	1.8094
Control C	40	2.3664	42	2.3923
13	3	5.9161	33	5.785
24	5	3.3910	8	3.3614
15	6	2.7314	7	2.7651
6	10	1.7225	46	1.7137
18	11	1.9190	25	1.9341
29	12	0.9627	21	0.9729
34	13	4.2248	26	4.2512
38	18	3.1665	29	3.1540
37	19	3.9695	43	3.9411
43	30	2.8476	39	2.7467
42	32	1.5040	36	1.4184

REFERENCES

[1] "WebMD," 2014. [Online]. Available: https://www.webmd.com/women/picture-of-the-breasts#1.

[2] "MedicineNet," 2016. [Online]. Available: https://www.medicinenet.com/script/main/art.asp?articlekey=2524.

[3] "The National Cancer Institute," 2017. [Online]. Available: https://www.cancer.gov/types/breast.

[4] "Cancer Treatment Centers of America," 2017. [Online]. Available: http://www.cancercenter.com/breast-cancer/.

[5] "American Joint Committee on Cancer," 2017. [Online]. Available: https://cancerstaging.org/Pages/default.aspx.

[6] "BreastCancer.org," 2017. [Online]. Available: http://www.breastcancer.org/.

[7] "The American Cancer Society," 2017. [Online]. Available: https://www.cancer.org/cancer/breast-cancer.html.

[8] S. Goyal, "Current Application and Research Directions for Partial-Breast Irradiation," *Oncology*, vol. 21, no. 4, 2007.

[9] C. Nijeh, "Accelerated PartialBreast Irradiation (APBI): A review of aviable techniques," *Radiation Oncology*, vol. 5, no. 90, 2010.

[10] M. Poggi, "Eighteen-year results in the treatment of early breast carcinoma with mastectomy versus breast conservation therapy: the National Cancer Institute Randomized Trial.," *National Center for Biotechnology Information, U.S. National Library of Medicine*, pp. 697-702, 15 August 2003.

[11] C. Washington, Principles and Practice of Radiation Therapy, Elsevier Health Sciences, 2015.

[12] D. Wazer, Accelerated Partial Breast Irradiation: Techniques and Clinical Implementation, Springer, 2006.

[13] C. Shah, "The American Brachytherapy Society consenus statement for Accelerated Partial Breast Irradiation," *Brachytherapy*, pp. 267-277, 2013.

[14] ASBS Board of Directors, "Consensus Statement for Accelerated Partial Breast Irradiation," *The American Society of Breast Surgeons*, pp. 1-3, Revised 2011.

[15] American Society for Therapeutic Radiation Oncology, "Accelerated Partial Breast Irradiation: Executive summary for the update of an ASTRO Evidence-Based Consensus Statement," *Practical Radiation Oncology*, pp. 73-79, 2016.

[16] NSABP B-39, RTOG 0413, "A Randomized Phase III Study of Conventional Whole Breast Irradiation (WBI) Versus Partial Breast Irradiation (PBI) for Women with Stage 0, I, or II Breast Cancer," 2011.

[17] American College of Radiation Oncology, Statement on Partial Breast Irradiation, 2008.

[18] "BreastCancer.org," 2017. [Online]. Available: http://www.breastcancer.org/.

[19] J. Skowronek, "Brachytherapy in accelerated partial breast irradiation (APBI) – review," *Jounal of Contemporary Brachytherapy,* vol. 4, no. 3, pp. 152-164, 2012.

[20] M. Rivard, "Update of AAPM Task Group No. 43 Report: A revised AAPM protocol for brachytherapy dose calculations," *Medical physics,* vol. 31, no. 3, pp. 633-674, 2004.

[21] "Cianna Medical," 2017. [Online]. Available: https://www.ciannamedical.com/.

[22] R. Chen, Theory of Thermoluminescence and Related Phenomena, World Scientific, 1997.

[23] T. H. Blair, Energy Production Systems Engineering, John Wiley & Sons, 2016.

[24] J. Cameron, "Radiation Dosimetry," *Environmental Health Perspectives,* vol. 91, pp. 45-48, 1991.

[25] W. Hendee, Radiation Therapy Physics 3rd Ed., John Wiley and Sons, Inc., 2005.

[26] P. Mayles, Handbook of Radiotherapy Physics: Theory and Practice, Taylor & Francis Group, LLC, 2007.

[27] F. Khan, The Physics of Radiation Therapy 4th Ed., Lippincott Williams & Wilkins, 2010.

[28] R. Varela, *TLD Theoretical Information,* Revised 2012.

[29] C. Furetta, Handbook of Thermoluminescence, World Scientific Publishing Co., 2002.

[30] J. Raffi, "Determination of exit skin dose for Ir-192 intracavitary accelerated partial breast irradiation with thermoluminescent dosimeters," *Medical Physics,* vol. 37, no. 6, p. 2693–2702, 2010.

[31] S. Richardson, "Dosimetric Comparison of TG-43 Formalism with Brachyvision Acuros and Monte Carlo Method for Patients Treated with the Savi Partial Breast Applicator," *Brachytherapy*, vol. 12, no. 22-23, 2013.

[32] M. Lamberto, "Dosimetric Impact of SAVI Breast Applicator Position Near Tissue Heterogeneities," *Brachytherapy*, vol. 15, p. S164, 2016.

[33] S. Sample, "A Realistic Analysis of Dose Enhancement in a SAVI Applicator," in *Radiological Society of North America 2009 Scientific Assembly and Annual Meeting*, 2009.

[34] S. Richardson, "Dosimetric effects of an air cavity for the SAVI™ partial breast irradiation applicator," *Medical Physics*, vol. 37, no. 8, pp. 3919-3926, 2010.